

1 **Methane Combustion in MILD Oxyfuel Regime: Influences of Dilu-**  
2 **tion Atmosphere in Co-flow Configuration**

3

4 Sheng Chen <sup>\*1,2,3</sup>, Hao Liu <sup>1</sup>, Chuguang Zheng <sup>1</sup>

5 1. State Key Laboratory of Coal Combustion, Huazhong University of Science  
6 and Technology, Wuhan 430074, China

7 2. Institute for Modelling and Simulation in Fluodynamics, Nanoscience and  
8 Industrial Mathematics "Gregorio Millán Barbany", Universidad Carlos III  
9 de Madrid, Leganes 28911, Spain

10 3. Faculty of Engineering, The University of Nottingham, University Park,  
11 Nottingham NG7 2RD, UK

12 Corresponding author. Faculty of Engineering, University of Nottingham. E-  
13 mail address: shengchen.hust@gmail.com (Sheng Chen)

14

15 **Abstract:** MILD (moderate or intense low oxygen dilution) oxyfuel com-  
16 bustion is a recently proposed clean combustion mode which can remedy  
17 the shortcomings of the standard oxyfuel combustion technology. Nowadays  
18 most available studies on MILD oxyfuel combustion focus on how to realize  
19 this new combustion regime in  $O_2/CO_2$  atmosphere. The open research on  
20 methane MILD oxyfuel combustion in  $O_2/H_2O$  atmosphere is quite sparse. In  
21 the present work, we carry out a comprehensive comparison study on methane  
22 MILD oxyfuel combustion in different dilution atmosphere for the first time.

23 The JHC (jet in hot co-flow) burner is adopted as a research prototype. The  
24 investigation is based on numerical simulation, so firstly the adopted numer-  
25 ical approach is validated by some experimental data in open literature. The  
26 numerical comparison is conducted by varying the mass fraction of oxygen  
27 in the co-flow and the temperature of the hot co-flow, two key parameters  
28 affecting fine reaction structures in JHC. Through the present investigation,  
29 a number of findings are reported for the first time and some conclusions pre-  
30 sented in previous publications are checked with analyses, especially on some  
31 conflicted claims between the previous publications. In addition, several new  
32 questions are raised, which may inspire further research activities in future.

33 Keywords: MILD combustion; Oxyfuel combustion; Methane; CO<sub>2</sub>-dilution;  
34 H<sub>2</sub>O-dilution; oxy-steam

35

## 36 **1 Introduction**

37 MILD oxyfuel combustion [1,2] is a recently emerging term which can be re-  
38 garded as an organic combination of two promising clean combustion technolo-  
39 gies, MILD (moderate or intense low oxygen dilution) combustion and oxyfuel  
40 combustion. Originally, some of the present authors proposed this new idea in  
41 order to utilize biogas with a higher efficiency [3]. Soon after, it was extended  
42 to various fuels [2,4–8]. Through these preliminary studies, it was found that

43 the MILD combustion regime could be established more easily in oxyfuel con-  
44 dition [1,3,7] and meanwhile a number of shortcomings of the standard oxyfuel  
45 combustion technology could be remedied straightforwardly by the introduc-  
46 tion of MILD combustion regime [4]. Especially, the experimental efforts [4,7]  
47 further demonstrated there was no obvious technical difficulty to establish  
48 and to sustain MILD oxyfuel combustion in industrial furnaces. Consequent-  
49 ly, MILD oxyfuel combustion may become one of the next generation clean  
50 combustion technologies for carbon capture which is crucial to the sustainable  
51 development of human society [9]. For this purpose, consecutive research on  
52 MILD oxyfuel combustion is essential as our knowledge, as well as available  
53 open literature, on it is quite limited [1,2].

54 Originally, the research on MILD oxyfuel combustion focused on how to realize  
55 this new combustion regime in  $O_2/CO_2$  atmosphere, namely oxygen in oxidan-  
56 t flow being diluted by carbon dioxide rather than nitrogen in conventional  
57 air-firing mode [2,4–8]. Recently, the present authors discussed the possibility  
58 to establish and to sustain MILD oxyfuel combustion in  $O_2/H_2O$  atmosphere  
59 where oxygen in oxidant flow is diluted by steam rather than carbon dioxide  
60 [1]. As shown in Ref.[1], compared with its  $O_2/CO_2$  counterpart, there are  
61 at least three advantages to realize MILD oxyfuel combustion in  $O_2/H_2O$  at-  
62 mosphere, such as simpler plant configuration, lower operation cost and high  
63 power-generation efficiency. In the oxyfuel combustion research community,  
64 the approach to realize oxyfuel combustion in  $O_2/H_2O$  atmosphere is named

65 as steam-moderated oxyfuel combustion or oxy-steam combustion [1,10]. As  
66 the chemical and physical properties of steam are quite different from those of  
67  $\text{CO}_2$ , inevitably, compared with its  $\text{O}_2/\text{CO}_2$  counterpart, combustion behavior  
68 may be significantly altered in the steam-moderated oxyfuel scenario. Conse-  
69 quently, comprehensive comparison of combustion characteristics between in  
70  $\text{O}_2/\text{CO}_2$  and in  $\text{O}_2/\text{H}_2\text{O}$  atmosphere is necessary, as it has done between in  
71  $\text{O}_2/\text{CO}_2$  (standard oxyfuel combustion) and in  $\text{O}_2/\text{N}_2$  (air-firing mode) con-  
72 dition [11]. Unfortunately, nowadays the essential studies on this critical topic  
73 are extremely sparse. Some of the present authors compared the effects of  
74  $\text{CO}_2$ - and  $\text{H}_2\text{O}$ -dilution on combustion temperature and reaction kinetics of  
75 methane [12]. It was observed that the chemical and thermal effects of  $\text{CO}_2$   
76 and of  $\text{H}_2\text{O}$  on combustion behavior of methane are quite different and conse-  
77 quently they will alter combustion temperature and reaction paths of methane  
78 in the oxyfuel combustion regime by different ways. Zou et al. investigated  
79 steam's effect on temperature distribution in methane oxy-steam combustion  
80 [13]. With the aid of numerical simulation, they found out the key elementary  
81 reaction step which determined the combustion temperature. In Refs.[14–16],  
82 wet recycle of oxy-coal combustion was investigated, not only by numerical  
83 simulation but also by experimental approaches. As steam is rich in wet re-  
84 cycle of oxyfuel combustion, it was observed that high concentration  $\text{H}_2\text{O}$  in  
85 recycled flue gas could influence combustion characteristics of pulverized coal  
86 significantly [14–16]. However, these studies [12–16] all are limited in the so-  
87 called "feed-back" combustion regime rather than MILD combustion regime

88 [1], so whether the conclusions made in these studies are tenable in the MILD  
89 oxyfuel combustion regime is still an open question. To the best knowledge of  
90 the present authors, on comparison study between CO<sub>2</sub> and H<sub>2</sub>O on estab-  
91 lishing and sustaining MILD oxyfuel regime, until now perhaps there are only  
92 three open publications [1,16,17]. In Ref.[1], the present authors compared  
93 the effects of CO<sub>2</sub> and of H<sub>2</sub>O on establishing biogas MILD oxyfuel combus-  
94 tion with the aid of a counter-flow configuration. It was found that biogas  
95 MILD oxy-fuel combustion would be established more easily in O<sub>2</sub>/H<sub>2</sub>O at-  
96 mosphere but meanwhile the reaction zone would become more complicated.  
97 Sabia et al. discussed propane auto-ignition delay time in MILD combustion  
98 regime, where reactants were diluted by CO<sub>2</sub> and H<sub>2</sub>O, respectively [16]. In  
99 Ref.[16], a cross-flow configuration was adopted. The authors claimed that in  
100 the O<sub>2</sub>/H<sub>2</sub>O option the auto-ignition delay time would be a little shorter than  
101 its O<sub>2</sub>/CO<sub>2</sub> counterpart. Recently, some of the present authors conducted a  
102 numerical investigation about the influence of H<sub>2</sub>O addition on MILD oxy-coal  
103 combustion [17]. The concentration of H<sub>2</sub>O in oxidant flow varied from 0% (s-  
104 tandard O<sub>2</sub>/CO<sub>2</sub> condition) to 70% (oxy-steam atmosphere). It was observed  
105 that NO emission could be suppressed and heat transfer would be enhanced  
106 in O<sub>2</sub>/H<sub>2</sub>O atmosphere. As the IFRF (International Flame Research Founda-  
107 tion) semi-industrial scale co-flow furnace adopted in Ref.[17] is not an ideal  
108 MILD oxyfuel combustion research prototype and the extreme complication  
109 of coal combustion, Ref.[17] failed to reveal the influence of different types of  
110 dilution gases (H<sub>2</sub>O or CO<sub>2</sub>) on fine reaction structures. In our latest work

111 [1], it has been underlined that further research on this topic is necessary as  
112 co-flow is more popularly found in practical combustion systems. Especially,  
113 through our recent research [12,19], it was observed that the effect of dilution  
114 gas on combustion performance in a co-flow configuration may differ from its  
115 counter-flow counterpart because flow-reaction interaction, which is exclud-  
116 ed in a one-dimension model (e.g. a counter-flow configuration), will play an  
117 important role in a co-flow configuration. Consequently, in order to deepen  
118 our knowledge in this emerging area so to advance its application in energy  
119 industry, a systematic comparison between the performance of co-flow MILD  
120 oxyfuel combustion in  $O_2/H_2O$  condition and that in  $O_2/CO_2$  atmosphere, is  
121 essential.

122 In order to bridge the aforementioned gap, in this work we numerically investi-  
123 gate methane combustion in MILD oxyfuel regime, diluted by carbon dioxide  
124 and steam, respectively. The JHC (jet in hot co-flow) burner developed in  
125 Ref.[20] is adopted in the present study as the research prototype. Besides the  
126 JHC burner proposed by Dally's group[20], there is another popularly used  
127 JHC burner developed by the researchers in Delft[21,22]. Within a JHC burn-  
128 er the influence of surrounding atmosphere on fine reaction structures can  
129 be prevented, so it is an ideal benchmark for a comparison study on MILD  
130 oxyfuel combustion in various dilution gases. The investigation is based on  
131 numerical simulation, so firstly the adopted numerical approach is validated  
132 by the experimental data [20]. In the present work, besides the influences of

133 various dilution atmospheres, the effects of temperature of co-flow on MILD  
134 oxyfuel combustion are also investigated as until now no open effort report-  
135 ed on this important issue. Through the present study, a number of findings  
136 are reported for the first time and some conclusions presented in previous  
137 publications are checked with analyses on the differences, especially on some  
138 conflicted claims. In addition, several new questions are raised, which may  
139 inspire future research activities.

## 140 **2 Computational Details**

### 141 *2.1 Configuration of the JHC burner and numerical conditions*

142 The configuration of the JHC burner is illustrated by Fig.1 and the detailed  
143 description on it please refer to Ref.[20]. As the JHC burner is axisymmetric,  
144 in order to reduce numerical simulation cost, the investigated domain can be  
145 simplified as a two-dimensional case, as shown by Fig. 2. In the JHC burner,  
146 fuel is injected through the central jet pipe whose inner diameter reads 4.25  
147 mm. The fuel jet pipe is surrounded by an annulus oxidant co-flow pipe with  
148 an inner diameter 77.75 mm. The whole JHC burner is operated inside a wind  
149 tunnel filled by environmental gas. The velocity boundary condition is adopt-  
150 ed for all jet flows and at the downstream exit the pressure outlet boundary  
151 condition is assumed. In addition, a zero-shear stress wall boundary condition  
152 is employed as the tunnel flow is much wider than the jet flows. Because the

153 JHC burner is originally designed for air MILD combustion research rather  
154 than MILD oxyfuel combustion, in the present simulation, we replace air in  
155 tunnel flow by steam or carbon dioxide, respectively. Furthermore, the tem-  
156 perature of tunnel flow is set as 400 K to guarantee H<sub>2</sub>O at its steam status  
157 in tunnel flow. Finally, to reduce the complication induced by variation of fuel  
158 mixture, in the present work it is assumed that the fuel jet flow consists of  
159 pure methane, instead of the mixture of methane and hydrogen used in Re-  
160 f.[20]. Table 1 lists the detailed information of investigated cases covered by  
161 the present simulation. In Table 1,  $\mathbf{u}$  and  $T$  represent jet flow velocity and  
162 temperature, respectively. The mass fraction of reactants is also listed in the  
163 Table. As the present study aims at the effects of temperature and oxygen  
164 concentration of co-flow on methane MILD oxyfuel combustion in different  
165 dilution atmosphere, these two parameters vary over a wider range (the tem-  
166 perature of the co-flow  $1500 \leq T_{cof} \leq 2100$  and the oxygen mass fraction  
167 in the co-flow  $6\% \leq f_{o2} \leq 18\%$ ). Through a numerical test, it is found that  
168 reactants can not be ignited successfully if oxygen mass fraction in the co-flow  
169 is lower than 6% or the temperature of the co-flow is less than 1500 K. It is an  
170 obvious difference from the air MILD combustion [20] and it may result from  
171 two aspects: (1) there is no hydrogen addition in the present fuel flow while  
172 hydrogen is more active than methane to establish and to sustain combustion;  
173 (2) the specific heat capacity of H<sub>2</sub>O, as well as that of CO<sub>2</sub>, is larger than  
174 air.



176 The present numerical simulation is conducted with the aid of the commercial  
177 CFD software FLUENT (version 6.3) to solve the Reynolds Averaged Navier-  
178 Stokes (RANS) equations for turbulence [23]. For heat radiation calculation,  
179 the discrete ordinate (DO) model is used [23]. In addition, a modified weighted  
180 sum of gray gas (WSGG) model is adopted to calculate the gas mixture total  
181 emissivity [19]. Finally, the eddy dissipation concept (EDC) model [23] with  
182 detailed chemical kinetic mechanisms (GRI-Mech 3.0, excluding the reactions  
183 relevant to Nitrogen) [24] is employed for turbulence-reaction interaction and  
184 reaction kinetics. In the present numerical research, 46560 cells are employed,  
185 as illustrated by Fig.2, which is the same as that used in Ref.[19]. As demon-  
186 strated by our recent work [19], such grid resolution is fine enough to obtain  
187 grid-independent numerical prediction. The detailed information about grid  
188 discretization and numerical convergence please refer to our previous work  
189 [19].

190 Because there is no open experimental data on the JHC oxyfuel MILD com-  
191 bustion cases investigated in the present work, we validate the reliability and  
192 accuracy of the present numerical approach by the JHC air MILD combustion  
193 experiments conducted in Ref.[20]. Fig. 3 illustrates the comparison of temper-  
194 ature and species, along the radial direction, between the present numerical  
195 prediction and the experimental measurements of JHC air MILD combustion

196 with 3%, 6%, and 9% oxygen mass fraction in the co-flow at the axial location  
197  $x = 30$  mm [20]. For the measured CO hump in the co-flow stream, it was  
198 explained to be the result of cooling and extinction of the secondary flame  
199 near the burner outer wall [19,20]. The present prediction agrees well with the  
200 experimental data for these three JHC MILD flames, which demonstrates the  
201 present numerical approach is adequate for modeling JHC combustion.

### 202 **3 Results and Discussion**

203 As shown in previous research[2,6,19], for JHC combustion, the temperature of  
204 the co-flow ( $T_{cof}$ ) and the oxygen mass fraction in the co-flow ( $f_{o2}$ ) are the key  
205 parameters that affect fine reaction structures. Therefore, in the present work  
206 we compare the MILD oxyfuel combustion characteristics in different dilution  
207 atmosphere by adjusting these two parameters, respectively. Firstly we try  
208 to reveal the MILD oxyfuel combustion characteristics in different dilution  
209 atmosphere with a changeable  $f_{o2}$  and a fixed  $T_{cof}$ . In succession,  $T_{cof}$  varies  
210 with a constant  $f_{o2}$ .

#### 211 *3.1 Comparison against various oxygen concentration $f_{o2}$ in co-flow*

212 In order to compare the effects of oxygen mass fraction in the co-flow ( $f_{o2}$ ) on  
213 combustion behavior in different dilution conditions, the cases at  $T_{cof} = 1800$   
214 K and  $6\% \leq f_{o2} \leq 18\%$  are chosen as the representatives in this section.

215 Figure 4 illustrates the temperature distribution in  $O_2/H_2O$  or  $O_2/CO_2$  atmo-  
216 sphere, respectively. According to this figure, it can be observed that there are  
217 two common features between  $H_2O$ - and  $CO_2$ -dilution condition: (1) the max-  
218 imum temperature of the reactants will increase when more oxygen is added  
219 into the co-flow; (2) the zone with high temperature will expand towards the  
220 exit as  $f_{o_2}$  increases. These phenomena are expected as combustion will be  
221 enhanced with more oxygen. Meanwhile, the differences between them are al-  
222 so obvious: (1) their maximum temperatures are not identical; and (2) their  
223 temperature profiles are quite different. The details are discussed below.

224 Figure 5 plots the maximum temperature ( $T_{max}$ ) and temperature rise ( $\Delta T$ ) of  
225 the reactants in  $O_2/H_2O$  or  $O_2/CO_2$  condition, respectively. In both dilution  
226 atmosphere,  $T_{max}$ , as well as  $\Delta T$ , is almost a linear increasing function of  
227  $f_{o_2}$ . As shown by Fig. 5(b), the temperature rise of the reactants is lower  
228 than the ignition temperature of methane and the temperature of co-flow is  
229 above the ignition temperature of methane, so the reactants react in the MILD  
230 oxyfuel regime [1,25]. The peak temperature in  $O_2/CO_2$  condition is always  
231 higher than its steam counterpart. In addition, the increasing rate of  $T_{max}$   
232 in  $O_2/CO_2$  condition is faster, so the gap between  $T_{max}$  in different dilution  
233 atmosphere becomes wider with  $f_{o_2}$  growing up. It mainly results from that  
234 the mass specific heat capacity of  $H_2O$  is larger than  $CO_2$ . Furthermore, the  
235 dilution gas may alter reaction paths by different ways, especially in relation  
236 to dissociation reactions, which also will influence heat release in combustion,

237 as discussed in our previous studies [1,12,19]. As shown in our latest work[1],  
238 the exothermic reaction chain of methane will be suppressed in oxy-steam  
239 atmosphere, depending on local temperature.

240 It has been reported that compared with its air-firing counterpart, in MILD  
241 oxyfuel combustion oxidization of fuels will take place within a larger area  
242 [2,6]. As shown in Refs. [2,6], in  $O_2/CO_2$  condition, the zone with intensive  
243 heat release will expand toward the exit of JHC. In our simulation, this phe-  
244 nomenon is observed, too. According to Fig. 4, it can be observed that the  
245 zone with high temperature will expand towards the exit in both  $O_2/CO_2$   
246 and  $O_2/H_2O$  condition. Especially, we find that in  $O_2/CO_2$  atmosphere the  
247 zone will expand more quickly. However, in its steam dilution counterpart,  
248 the zone with high temperature will expand obviously not only axially but  
249 also radially. In other words, in oxy-steam condition, most heat is released in  
250 the area closer to the fuel jet nozzle. It is another discovery reported by the  
251 present work for the first time. In all available open literature on MILD oxyfu-  
252 el combustion [1,2,4-8,16,17], few pay attention to compare reaction structure  
253 alteration between in  $CO_2$ - and in  $H_2O$ -dilution condition until the present  
254 work. This new finding is very crucial for burner and chamber design as they  
255 both depend closely on temperature distribution. It is clearer with the aid of  
256 the distribution of hydroxyl radical (OH), as depicted by Fig. 6. Usually in the  
257 MILD combustion research community OH is used as a kind of marker for  
258 "flame" front region as MILD combustion is flameless [26]. As illustrated by

259 Fig. 6, in both dilution atmosphere the OH contours will expand with more  
260 oxygen being added, but their shape are completely different. The shape of  
261 OH contours in  $O_2/CO_2$  condition looks like dragonflies' wings (namely long  
262 and slender), which is similar with its air MILD combustion counterpart [27].  
263 However, the shape of OH contours in  $O_2/H_2O$  atmosphere looks like but-  
264 terflies' wings (namely relative wider but shorter), quite different from its air  
265 MILD combustion [27] and  $CO_2$ -dilution counterpart [6]. In the "feedback"  
266 oxy-steam combustion [14–16], whether there exists a similar feature is still  
267 an open question and we will try to answer it in our future work. As in the  
268 oxy-steam condition the "flame" front is closer to the fuel jet nozzle, it is eas-  
269 ier to establish the MILD oxyfuel regime in  $H_2O$ -dilution atmosphere. This  
270 conclusion agrees with that drawn from its counterflow counterpart [1]. Figure  
271 7 plots the maximum of OH concentration at various  $f_{O_2}$ . In both dilution at-  
272 mosphere, the maximum of OH concentration will ascend nearly linearly with  
273  $f_{O_2}$ . It is in the expectation that the maximum of OH in  $O_2/H_2O$  condition  
274 is larger than its  $O_2/CO_2$  counterpart since the production of OH will be en-  
275 hanced by  $H_2O$  addition, as explained in detail in our previous work [12]. In  
276 Ref. [12], a counter-flow combustion prototype was adopted and the research  
277 objective is "feed-back" oxyfuel combustion. The present work demonstrates  
278 that the conclusion for "feed-back" oxyfuel combustion can be extended to  
279 MILD oxyfuel combustion. With relative lower OH concentration, as well as  
280 dragonfly-wing-like OH distribution, in  $O_2/CO_2$  condition it is easier to sus-  
281 tain the MILD oxyfuel combustion regime across the whole domain, which is

282 consistent with the conclusion claimed in Ref.[1].

283 Figure 8 illustrates CO distribution at various  $f_{o_2}$ . In Ref.[6], Mei et al. dis-  
284 cussed the dimension of CH<sub>4</sub> JHC flame in O<sub>2</sub>/CO<sub>2</sub> condition and they sug-  
285 gested to use the contour of CO mass fraction  $f_{co} = 0.01$  as an indicator to  
286 visualize "flame" size. In this work we follow their suggestion. Through Fig. 6,  
287 one can observe the "flame" size in oxy-steam condition will grow dramatical-  
288 ly with more oxygen addition. However, in its O<sub>2</sub>/CO<sub>2</sub> counterpart, the size  
289 of "flame" will nearly not change with  $f_{o_2}$ . In Ref.[6], Mei et al. claimed that  
290 "flame" size would decreased against  $f_{o_2}$  in O<sub>2</sub>/CO<sub>2</sub> co-flow. Our observation  
291 is different from their claim but similar with that reported in Ref.[5] in which  
292 oxyfuel combustion in the IFRF semi-industrial scale furnace was investigat-  
293 ed. The difference between the present work and Ref.[6] results from that Mei  
294 et al. adopted a modified JHC configuration in their research. In Ref.[6], the  
295 cold tunnel flow in original JHC burner scheme was removed and replaced  
296 by hot co-flow. Consequently, the diameter of the hot co-flow jet in Ref.[6] is  
297 so wide that there is sufficient oxygen for combustion anywhere in the whole  
298 investigated domain. Accordingly, the consumption speed of CH<sub>4</sub> is mainly  
299 determined by reaction rate. It can be looked as a kinetic-controlled combus-  
300 tion. However, in the present work, the consumption speed of CH<sub>4</sub> depends  
301 not only on reaction rate but also on local available oxygen concentration s-  
302 ince in the present JHC configuration there is no oxygen in the tunnel flow. In  
303 other words, the combustion in the present work is diffusion-kinetic-controlled

304 where chemical kinetics and aerodynamics (turbulent mixing) compete with  
305 each other. No doubt, the combustion style investigated in the present work is  
306 much closer to real combustion situation than the modified JHC scheme in Re-  
307 f.[6]. It also can explain why the result obtain in the present study is consistent  
308 with that from the semi-industrial scale furnace [5]. Nowadays there appear  
309 a number of studies (please see [19] and references therein) in which a mod-  
310 ified JHC burner like that used in Ref.[6] was adopted as a co-flow research  
311 prototype. Through the present work, it is indicated that we should check  
312 carefully before extending the conclusions claimed in these studies to realistic  
313 co-flow combustion systems. To mimic a realistic MILD oxyfuel combustion  
314 system, the present settings may be better. In addition, through Fig. 8 it can  
315 be observed that the "flame" size in oxy-steam condition is generally smaller  
316 and closer to the fuel jet nozzle, in comparison with its  $O_2/CO_2$  counterpart.  
317 This observation is consistent with the above conclusion made from tempera-  
318 ture and OH distribution. In Ref. [6], it was observed that with more oxygen  
319 addition in the  $O_2/CO_2$  co-flow, the peak value of CO concentration within  
320 the reaction zone would increase, similar with its air-firing MILD combustion  
321 counterpart [20]. A comprehensive explanation on this phenomenon has been  
322 presented in Ref.[12]. Through the present work, we find such conclusion is  
323 also true in  $O_2/H_2O$  condition. In addition, as Ref.[12] focuses on "feed-back"  
324 oxyfuel combustion, through the present work it can be proved the above phe-  
325 nomenon is a common feature in oxyfuel combustion, regardless of dilution  
326 gases. In Ref.[2], it was reported that CO concentration would decrease slight-

327 ly against  $f_{o_2}$ . At first glance it seems that this conclusion is opposed to that  
328 in Refs. [6,20] and the present study. In fact, the conclusion in Ref.[2] was  
329 tenable within the mix layer (namely the network reactor illustrated by Fig.  
330 11 in Ref.[2]) rather than the whole domain of JHC [6,20]. As shown by Fig. 9,  
331 the CO maximum in both dilution atmosphere will grow almost linearly with  
332  $f_{o_2}$ . Whatever  $f_{o_2}$  is, the CO maximum in  $O_2/CO_2$  is always bigger than that  
333 in its oxy-steam counterpart. Especially, their gap will be enlarged with  $f_{o_2}$   
334 increasing. In our previous work [12], it was observed a similar phenomenon in  
335 counter-flow "feed-back" oxyfuel combustion. Consequently, it is also a com-  
336 mon feature of oxyfuel combustion. The detailed explanation on how  $H_2O$   
337 addition will suppress CO generation please refer to Ref.[12]. Figures 10-11  
338 plot the CO profiles at different axial positions  $x = 90$  and  $x = 120$  mm. The  
339 profiles in both  $O_2/CO_2$  and  $O_2/H_2O$  condition are similar with their air-firing  
340 counterpart: the gradient of CO concentration along radial direction becomes  
341 sharp with more oxygen addition [6,20]. Furthermore, it can be observed in  
342  $O_2/H_2O$  condition the gradient of CO concentration along radial direction is  
343 more gentle than its  $O_2/CO_2$  counterpart. This observation implies that in  
344 oxy-steam co-flow condition the MILD combustion regime can be established  
345 more easily, agreeing with the conclusion from the counter-flow configuration  
346 [1]. Moreover, in our previous study [28], it was found that the co-flow methane  
347 MILD combustion would be influenced significantly by the shape of furnace  
348 chamber. According to Figs.8, 10 and 11, one may conclude MILD combustion  
349 in oxy-steam condition is more flexible as the size of reaction zone in  $O_2/H_2O$



350 condition is smaller (especially at low oxygen concentration) and within the  
351 near-field of the fuel jet nozzle. Accordingly it will receive less effect than its  
352  $O_2/CO_2$  counterpart.

353 Figure 12 depicts the distribution of  $O_2$  with various  $f_{o_2}$ . One can observe that  
354 in the vicinity of the jet, the profiles of  $O_2$  in  $O_2/H_2O$  and  $O_2/CO_2$  condition  
355 are very similar, however their discrepancies become obvious in the far-field.  
356 It is more clear with the aid of Fig.13, where the profiles of  $O_2$  at  $x = 30$  mm  
357 (near-field) and  $x = 90$  mm (far-field) are illustrated. In the near-field, the  
358 profiles of  $O_2$  in both dilution atmosphere nearly overlap with each other. It  
359 agrees with the observation in Ref.[2] where only  $O_2/CO_2$  condition was con-  
360 sidered. In the far-field,  $O_2$  concentration in  $O_2/H_2O$  condition is always lower  
361 than its  $O_2/CO_2$  counterpart, which is consistent with Fig.10 and indicates  
362 oxidants are consumed faster in oxy-steam condition.

363 In Ref.[2], it was reported that in the near field ( $x = 30$  mm), the differences  
364 between the profiles of CO,  $O_2$  and OH in  $O_2/N_2$  atmosphere and those in  
365  $O_2/CO_2$  condition are very small. However, through the present work, it is  
366 observed that except  $O_2$ , there are obvious differences in most scalar distri-  
367 butions between in  $O_2/H_2O$  and in  $O_2/CO_2$  condition, even in the near field.  
368 Consequently, one should pay great attention on burner design for oxy-steam  
369 combustion due to its complicated reaction structures. This conclusion is con-  
370 sistent with that in Ref.[1].

371 The distribution of formyl (HCO) is shown by Fig.14. In the near-field of the  
372 fuel jet nozzle, HCO concentration will increase with more oxygen addition in  
373 both dilution atmosphere. In Ref.[6] it was reported in O<sub>2</sub>/CO<sub>2</sub> condition the  
374 peak value of HCO would grow up with  $f_{o_2}$ . The present results are consistent  
375 with it and prove this conclusion also can hold water in its oxy-steam counter-  
376 part. As HCO is an indicator for heat release during combustion [2,26], it can  
377 be concluded that heat release will be enhanced by increasing  $f_{o_2}$ . Moreover,  
378 HCO concentration in O<sub>2</sub>/CO<sub>2</sub> condition is always higher than its O<sub>2</sub>/H<sub>2</sub>O  
379 counterpart, as illustrated by Figs.14 and 16 (a), so in O<sub>2</sub>/CO<sub>2</sub> condition  
380 heat release intensity is higher than in oxy-steam atmosphere, which is con-  
381 sistent with Fig. 4. It can answer why MILD oxyfuel combustion is easier  
382 to be sustained in O<sub>2</sub>/CO<sub>2</sub> condition. In our previous work [12], it was also  
383 observed that HCO concentration in O<sub>2</sub>/H<sub>2</sub>O condition was lower than its  
384 O<sub>2</sub>/CO<sub>2</sub> counterpart, which resulted from that H<sub>2</sub>O addition would modify  
385 the chemical equilibrium of the reaction step R46. Through the present work,  
386 it can be proved the analysis in Ref.[12] where counter-flow prototype adopted  
387 still works well for JHC configuration. And it is a common feature between  
388 "feed-back" oxyfuel combustion and MILD oxyfuel combustion.

389 Figure 15 plots the distribution of formaldehyde (CH<sub>2</sub>O) which can serve as  
390 an indicator for ignition [2,26]. Since CH<sub>2</sub>O predominantly exists in low tem-  
391 perature condition, therefore the concentration of CH<sub>2</sub>O will decrease against  
392  $f_{o_2}$  increasing [6,26]. The present results agree with the conclusion in [6,26].

393 As shown by Fig.4, a higher  $f_{o_2}$  implies a higher combustion temperature. Be-  
 394 cause  $H_2O$  addition will suppress  $CH_2O$  generation [12], in oxy-steam atmo-  
 395 sphere  $CH_2O$  concentration in the near-field is a slightly lower than its  $O_2/CO_2$   
 396 counterpart. In  $O_2/CO_2$  condition, the profiles of  $CH_2O$  alter sensitively to  
 397 the variation of  $f_{o_2}$ , while in  $O_2/H_2O$  atmosphere the change is relatively  
 398 smaller. It implies the establishment of MILD combustion in  $O_2/H_2O$  condi-  
 399 tion receives less influence by oxygen fluctuation. Consequently, it is easier  
 400 to establish MILD combustion regime in oxy-steam condition. It is consistent  
 401 with the above analysis and the conclusion in Ref.[1]. Fig. 16 (b) depicts the  
 402 maximums of  $CH_2O$  in both dilution atmosphere. The peak value of  $CH_2O$  in  
 403  $CO_2$ -dilution atmosphere is always larger than its  $H_2O$ -dilution counterpart,  
 404 which is consistent with its counter-flow "feed-back" counterpart [12]. Togeth-  
 405 er with Fig.5, Fig. 16 (b) indicates that over the whole domain the uniformity  
 406 of ignition in oxy-steam is better than its  $CO_2$ -dilution counterpart.

### 407 3.2 Comparison against various temperature $T_{cof}$ of co-flow

408 In order to compare the effects of the temperature of the hot co-flow ( $T_{cof}$ ) on  
 409 combustion behavior in  $O_2/H_2O$  and  $O_2/CO_2$  condition, the cases at  $f_{o_2} = 9\%$   
 410 and  $1500K \leq T_{cof} \leq 2100K$  are chosen as the representatives in this section.

411 Figure 17 illustrates the temperature distribution in  $O_2/H_2O$  and  $O_2/CO_2$   
 412 condition at various  $T_{cof}$ . In  $CO_2$ -dilution condition, the maximum temper-

413 ature of the reactants will climb up with a higher  $T_{cof}$  and the zone with  
 414 high temperature will expand towards the exit as  $T_{cof}$  increases. The former  
 415 phenomenon has been reported in Ref.[6] and the latter one was also ob-  
 416 served in Ref.[2]. Refs.[2,6] just focused on  $O_2/CO_2$  atmosphere. Through the  
 417 present study, we can confirm these phenomena exist in oxy-steam condition,  
 418 too. However, the influences of variation of  $T_{cof}$  on the temperature field in  
 419  $O_2/H_2O$  and  $O_2/CO_2$  condition are quite different. The isotherms in these two  
 420 types of dilution atmosphere differ with each other obviously, especially in the  
 421 vicinity of the fuel jet nozzle. In addition, the high temperature zone expands  
 422 more quickly in  $CO_2$ -dilution atmosphere. The maximum temperature of the  
 423 reactants is illustrated by Fig.18.  $T_{max}$  is a monotonic increasing function of  
 424  $T_{cof}$  in both dilution conditions and since  $T_{cof} \geq 1600$  K  $T_{max}$  grows up almost  
 425 linearly.  $T_{max}$  in  $O_2/H_2O$  atmosphere is always smaller than its  $CO_2$ -dilution  
 426 counterpart. As mentioned above, it results from that the mass specific heat  
 427 capacity of  $H_2O$  is larger than  $CO_2$ . However, their gap will decrease against  
 428  $T_{cof}$  increasing, which implies a higher  $T_{cof}$  will improve the uniformity of  
 429 temperature field of MILD oxyfuel combustion in either dilution atmosphere.  
 430 This observation agrees with that presented in Ref.[6]. Moreover, making a  
 431 comparison between Figs. 4-5 and Figs.17-18, one may conclude the influence  
 432 of variation of  $f_{o_2}$  on the temperature field is more significant than  $T_{cof}$ .

433 The distribution of OH with various  $T_{cof}$  is depicted by Fig. 19. It can be  
 434 observed that the "flame" front region in oxy-steam atmosphere is more sen-

435 sitive to  $T_{cof}$ , in comparison with its  $O_2/CO_2$  counterpart. With a relative  
436 low co-flow temperature, such as  $T_{cof} = 1500$  K, the "flame" front region  
437 in oxy-steam atmosphere is much smaller than its  $O_2/CO_2$  counterpart. The  
438 shape of OH contours in  $H_2O$ -dilution condition looks like a dragonfly's wing,  
439 similar with its  $CO_2$ -dilution counterpart although the former is shorter. S-  
440 ince  $T_{cof} \geq 1600$  K, the "flame" front region in oxy-steam condition expands  
441 substantially along the radial direction and now the shape of OH contours  
442 in  $H_2O$ -dilution condition looks like a butterfly's wing, not resembling that  
443 in  $O_2/CO_2$  atmosphere any longer. And now the "flame" front region in the  
444 former is much larger than the latter. The sensitivity of OH generation to  
445  $T_{cof}$  in oxy-steam condition is also reflected by Fig.20. The maximum of OH  
446 concentration in  $O_2/H_2O$  condition ascends much faster than in  $O_2/CO_2$  at-  
447 mosphere. In our previous study on MILD oxyfuel counterflow combustion [1],  
448 it was found that the reaction structures in steam-dilution condition would be  
449 more complex than in  $O_2/CO_2$  atmosphere. The present work demonstrates  
450 such conclusion can apply to the co-flow scenario. Fig.20 illustrates the varia-  
451 tion of maximum of OH concentration at various  $T_{cof}$ . The maximum of OH  
452 concentration in either dilution atmosphere will grow up with  $T_{cof}$ , which is  
453 consistent with the result reported in Ref.[6]. As mentioned above, as the peak  
454 temperature in  $O_2/H_2O$  condition is lower than its  $O_2/CO_2$  counterpart, the  
455 maximum of OH concentration in the former is always higher than the latter.  
456 The increasing rate of the maximum of OH concentration in oxy-steam atmo-  
457 sphere is much faster than its  $CO_2$ -dilution counterpart, which also implies

458 the fine reaction structures in  $O_2/H_2O$  condition are more sensitive to  $T_{cof}$ ,  
459 in comparison with its  $O_2/CO_2$  counterpart. In our previous work [1], it was  
460 claimed that the MILD oxyfuel combustion regime was established more eas-  
461 ily in oxy-steam condition. Through Figs. 19-20, we find this conclusion may  
462 depend on  $T_{cof}$  in the present co-flow configuration. Only since  $T_{cof} > 1500$  K,  
463 in  $O_2/H_2O$  condition, the peak value of OH concentration is significantly larg-  
464 er than its  $O_2/CO_2$  counterpart and the "flame" front region is substantially  
465 wider than that in  $CO_2$ -dilution atmosphere. Consequently, in the present in-  
466 vestigated cases, only since  $T_{cof} > 1500$  K, it is sure that the MILD oxy-fuel  
467 combustion regime can be established more easily in  $O_2/H_2O$  atmosphere.

468 Figure 21 plots the distribution of CO with various  $T_{cof}$ . The iso-concentration  
469 lines of CO are affected significantly by the variation of  $T_{cof}$ , especially in oxy-  
470 steam condition. If taking the contour of CO mass fraction  $f_{co} = 0.01$  as an  
471 indicator to visualize the "flame" size, as mentioned above, one can observe  
472 that the "flame" size in  $O_2/H_2O$  atmosphere changes substantially with  $T_{cof}$ .  
473 When  $T_{cof} = 1500$  K, the "flame" size in  $H_2O$ -dilution condtion is much s-  
474 maller than its  $CO_2$ -dilution counterpart. Then the "flame" size in the former  
475 atmosphere grows quickly with  $T_{cof}$  increasing. While  $T_{cof} = 2100$  K, the  
476 "flame" size in both dilution conditions is almost the same. On the contrary,  
477 although the CO iso-concentration lines in  $O_2/CO_2$  condition will alter obvi-  
478 ously with  $T_{cof}$ , the "flame" size in  $CO_2$ -dilution atmosphere grows slightly.  
479 The maximum of CO is depicted by Fig. 22. It is clear that the maximum

480 of CO will ascend with a higher  $T_{cof}$ , which is consistent with the conclusion  
481 given in Ref.[6]. In Ref.[6] only O<sub>2</sub>/CO<sub>2</sub> atmosphere was investigated. The  
482 present work shows there is a similar trend in oxy-steam condition. However,  
483 the increasing rate of the peak value of CO in O<sub>2</sub>/H<sub>2</sub>O condition is much  
484 slower than its O<sub>2</sub>/CO<sub>2</sub> counterpart. Taking Figs. 9 and 22 together, one can  
485 conclude that a crucial issue to guarantee the performance of MILD oxyfuel  
486 combustion in O<sub>2</sub>/CO<sub>2</sub> atmosphere is to ensure fuel to burn out in a finite  
487 room as the maximum of CO concentration at the outlet of the investigated  
488 domain will jump up quickly, exceeding 10%, with the fluctuation of either  
489  $T_{cof}$  or  $f_{o2}$ . Such high value of CO concentration at the outlet implies an  
490 extremely low combustion efficiency. On the contrary, in the oxy-steam con-  
491 dition, the maximum of CO concentration at the outlet of the investigated  
492 domain is always less than 4%, no matter whatever  $T_{cof}$  and  $f_{o2}$  are. From  
493 this viewpoint, burner and chamber design, which can improve aerodynamics  
494 in furnace and accordingly improve combustion efficiency, is more critical for  
495 operation in CO<sub>2</sub>-dilution condition.

496 Figure 23 shows the CO radial profiles at  $x = 90$  mm. In Ref.[29], it was  
497 reported that, in air MILD condition, the peak value of CO concentration  
498 along the radial direction would grow up with  $T_{cof}$  increasing. The present  
499 work proves such conclusion can be extended to MILD oxyfuel regime. In  
500 addition, a higher  $T_{cof}$  will sharpen the gradient of CO concentration in both  
501 dilution conditions. A similar observation was reported in Ref.[6] where only

502 O<sub>2</sub>/CO<sub>2</sub> atmosphere was investigated. Through the present work, it is found  
503 the radial gradient of CO concentration in O<sub>2</sub>/H<sub>2</sub>O is always much smaller  
504 than its CO<sub>2</sub>-dilution counterpart, no matter whatever  $T_{cof}$  is. The results  
505 reveal that the potential performance of MILD oxyfuel combustion in O<sub>2</sub>/H<sub>2</sub>O  
506 condition may be better than its O<sub>2</sub>/CO<sub>2</sub> counterpart not only along the axial  
507 direction but also along the radial direction of a chamber as in oxy-steam  
508 condition most fuel can be burnt out in a relative small zone, in comparison  
509 with its CO<sub>2</sub>-dilution counterpart.

510 The O<sub>2</sub> distribution with various  $T_{cof}$  is plotted by Fig. 24. Generally, the  
511 variation of  $T_{cof}$  will alter O<sub>2</sub> distribution significantly in both dilution atmo-  
512 sphere, especially in the far-field. Against  $T_{cof}$  increasing, O<sub>2</sub> concentration  
513 near the exit will decrease as a higher  $T_{cof}$  will intensify chemical reactions.  
514 Near the fuel jet nozzle, the influence of variation of  $T_{cof}$  on O<sub>2</sub> distribution is  
515 slight, as illustrated by Fig.25. In Ref.[29], it was also found that, in methane-  
516 air MILD combustion, O<sub>2</sub> distribution in the near-field is insensitive to  $T_{cof}$ .  
517 Through the present work, one may conclude that it is a common feature of  
518 methane MILD JHC combustion, regardless of dilution atmosphere. Taking  
519 Figs. 13 and 24 together, it can be observed that for any  $T_{cof}$  and  $f_{o2}$ , in  
520 the far-field the O<sub>2</sub> radial concentration in O<sub>2</sub>/H<sub>2</sub>O condition is always low-  
521 er than its O<sub>2</sub>/CO<sub>2</sub> counterpart. Such observation demonstrates once again  
522 that in oxy-steam condition the "flame" size is smaller than its CO<sub>2</sub>-dilution  
523 counterpart.



524 Figure 26 illustrates HCO profiles in O<sub>2</sub>/H<sub>2</sub>O and O<sub>2</sub>/CO<sub>2</sub> atmosphere, re-  
 525 spectively. HCO concentration will increase with a higher  $T_{cof}$  in both dilution  
 526 atmosphere as heat release will be enhanced by a hotter co-flow. A similar phe-  
 527 nomenon was also observed in methane-air MILD combustion [29]. No matter  
 528 whatever  $T_{cof}$  is, HCO concentration in O<sub>2</sub>/CO<sub>2</sub> condition is always higher  
 529 than its O<sub>2</sub>/H<sub>2</sub>O counterpart, as shown by Fig.27 (a). At a relative low co-  
 530 flow temperature ( $T_{cof} = 1500$  K), one can observe HCO concentration in  
 531 oxy-steam atmosphere is rarefied. According to Fig. 27, it can be observed  
 532 that in oxy-steam condition the variation of OH concentration versus  $T_{cof}$  is  
 533 "smooth", which also can be reflected by Fig. 26 (a). However, it is not true  
 534 for its O<sub>2</sub>/CO<sub>2</sub> counterpart. As shown by Fig. 26 (b), when  $T_{cof} < 1700$ , the  
 535 peak value of HCO at  $x = 30$  mm will increase quickly with  $T_{cof}$ , but since  
 536  $T_{cof} \geq 1700$ , the change becomes slow. It agrees with the results depicted  
 537 by Figs.19 and 21. Through these figures, one can observe that in O<sub>2</sub>/CO<sub>2</sub>  
 538 condition the shapes of OH, CO and HCO contours in the near-field change  
 539 significantly when  $T_{cof}$  rises from below 1700 K to above 1700 K. It implies  
 540 there appears a substantial change of the reaction structure in CO<sub>2</sub>-dilution  
 541 atmosphere. In other words, the MILD oxyfuel combustion performance in  
 542 O<sub>2</sub>/CO<sub>2</sub> condition is more sensitive to  $T_{cof}$ .

543 The radial distribution of CH<sub>2</sub>O in the near-field is plotted by Fig.28. In Re-  
 544 f.[29], it was found in the near-field of air MILD combustion the maximum  
 545 of CH<sub>2</sub>O concentration along the radial direction would decrease against  $T_{cof}$

546 growing up . The present results show this conclusion can be extended to CO<sub>2</sub>-  
547 dilution MILD oxyfuel combustion. However, it is not true in MILD oxy-steam  
548 condition. In O<sub>2</sub>/H<sub>2</sub>O atmosphere, there will appear two obvious peak values  
549 of CH<sub>2</sub>O concentration along the radial direction while in Ref.[29] only one was  
550 observed. In O<sub>2</sub>/CO<sub>2</sub> condition, the second peak of CH<sub>2</sub>O distribution along  
551 the radial direction is not as obvious as that in its H<sub>2</sub>O-dilution counterpart.  
552 This phenomenon implies in oxy-steam atmosphere the ignition of reactants  
553 will take place over a wider range than in O<sub>2</sub>/CO<sub>2</sub> or O<sub>2</sub>/N<sub>2</sub> condition. Fur-  
554 thermore, it also indicates the effect of  $T_{cof}$  on ignition is more complicated  
555 in H<sub>2</sub>O-dilution condition. In addition, in Ref.[29], it was observed that the  
556 "sharp angle" of the CH<sub>2</sub>O profile at a low  $T_{cof}$  (e.g.  $T_{cof} = 1500$  K) will be  
557 flattened by a high  $T_{cof}$  (e.g.  $T_{cof} = 1800$  K). Although it was observed firstly  
558 in methane-air MILD combustion, the present work reveals that this conclu-  
559 sion is also tenable in the MILD oxyfuel combustion regime, either diluted by  
560 CO<sub>2</sub> or by H<sub>2</sub>O. Such phenomenon indicates chemical reaction will become to  
561 vary mildly as  $T_{cof}$  increasing, which is consistent with the available research  
562 on high temperature air combustion [30].

## 563 4 Conclusion

564 In order to deepen our insight into MILD oxyfuel combustion, a recently e-  
565 merging idea for next generation clean combustion technology, in the present

566 work we carry out a comprehensive comparison study on methane MILD oxy-  
567 fuel combustion in different dilution atmosphere ( $O_2/H_2O$  and  $O_2/CO_2$ ). The  
568 JHC burner is adopted as a research prototype. The comparison is conducted  
569 by varying the mass fraction of oxygen in the co-flow ( $f_{o_2}$ ) and the temperature  
570 of the hot co-flow ( $T_{cof}$ ), two key parameters affecting fine reaction structures  
571 in JHC. The literature survey demonstrates the present work is a pioneering  
572 effort in this field.

573 Through the present study, a number of findings are reported for the first time  
574 and it is found the combustion characteristics in various dilution atmosphere  
575 are obviously different:

576 (1) In oxy-steam condition, the CO contours are affected more significantly  
577 by the variation of  $T_{cof}$  and  $f_{o_2}$ . But generally speaking, the "flame" size in  
578  $CO_2$ -dilution atmosphere is much larger than its  $O_2/H_2O$  counterpart. The  
579 maximum concentration of CO in  $O_2/CO_2$  atmosphere is about ten times  
580 large than its steam-dilution counterpart.

581 (2) In oxy-steam atmosphere the ignition of reactants will take place over a  
582 wider range than its  $O_2/CO_2$  or  $O_2/N_2$  counterpart. Especially, the effect of  
583  $T_{cof}$  on ignition is more complicated in  $H_2O$ -dilution condition.

584 (3) In general, it is easier to establish the MILD oxyfuel regime in  $H_2O$ -dilution  
585 atmosphere and in  $O_2/CO_2$  condition it is easier to sustain the MILD oxyfuel  
586 combustion regime across the whole domain. This conclusion agrees with that

587 drawn from its counter-flow counterpart investigated in our previous work [1].

588 (4) In Ref.[2], it was reported that in the near field of the JHC, the differences  
589 between the profiles of CO, O<sub>2</sub> and OH in O<sub>2</sub>/N<sub>2</sub> and in O<sub>2</sub>/CO<sub>2</sub> atmosphere  
590 are very small. However, through the present work, it is observed that ex-  
591 cept O<sub>2</sub>, there are obvious differences in most scalar distributions between in  
592 O<sub>2</sub>/H<sub>2</sub>O and in O<sub>2</sub>/CO<sub>2</sub> condition, even in the near field. Consequently, one  
593 should pay great attention on burner design for MILD oxy-steam combustion  
594 due to its complicated reaction structures.

595 Finally, several new questions are raised by the present study. For example,  
596 whether the shape of OH contours in "feed-back" oxyfuel combustion diluted  
597 by H<sub>2</sub>O will change from the dragon-wing-style to butterfly-wing-style? It is an  
598 important question as "feed-back" oxyfuel combustion diluted by H<sub>2</sub>O already  
599 appeared in industrial-scale furnaces [14–16] but until now nobody is aware  
600 of this issue. We will try to answer it in our future work since it will influence  
601 combustion performance, as shown by the present study.

## 602 **Acknowledgments**

603 This work has received funding from the Universidad Carlos III de Madrid, the  
604 European Unions Seventh Framework Programme for research, technological  
605 development and demonstration under grant agreement No. 600371, el Minis-  
606 terio de Economa y Competitividad (COFUND2014-51509), el Ministerio de

607 Educacin, cultura y Deporte (CEI-15-17) and Banco Santander. We also ac-  
608 knowledge the support from the British Newton Alumni Fellowship Scheme,  
609 the National Natural Science Foundation of China (Grant No. 51176061).

## 610 **References**

- 611 [1] Liu Y, Chen S, Yang B, Liu K, Zheng C. First and second thermodynamic-law  
612 comparison of biogas MILD oxy-fuel combustion moderated by CO<sub>2</sub> or H<sub>2</sub>O.  
613 Energy Conversion and Management 2015;106:625-634.
- 614 [2] Mardani A, Ghomshi AF. Numerical study of oxy-fuel MILD (moderate or  
615 intense low-oxygen dilution combustion) combustion for CH<sub>4</sub>-H<sub>2</sub> fuel. Energy  
616 2016;99:136-151
- 617 [3] Chen S, Zheng CG. Counterflow diffusion flame of hydrogen-enriched biogas  
618 under MILD oxy-fuel condition. International Journal of Hydrogen Energy  
619 2011;36:15403-15413.
- 620 [4] Li P, Dally BB, Mi J, Wang F. MILD oxy-combustion of gaseous fuels in a  
621 laboratory-scale furnace. Combust Flame 2013;160:933-946.
- 622 [5] Tu Y, Liu H, Chen S, Liu Z, Zhao H, Zheng C. Numerical study of combustion  
623 characteristics for pulverized coal under oxy-MILD operation. Fuel Processing  
624 Technology 2015;135: 80-90
- 625 [6] Mei ZF, Mi JC, Wang F, Zheng CG. Dimensions of CH<sub>4</sub>-Jet Flame in Hot  
626 O<sub>2</sub>/CO<sub>2</sub> Coflow. Energy Fuels 2012; 26: 3257-3266.

- 627 [7] Zhang J, Mi JC, Li P, Wang F, Dally BB. Moderate or Intense Low-Oxygen  
628 Dilution Combustion of Methane Diluted by CO<sub>2</sub> and N<sub>2</sub>. Energy Fuels 2015;29  
629 : 4576C4585
- 630 [8] Liu R, An E, Wu K, Liu Z. Numerical simulation of oxy-coal MILD  
631 combustion with high-velocity oxygen jets. Journal of the Energy Institute  
632 (2015), <http://dx.doi.org/10.1016/j.joei.2015.11.002>
- 633 [9] Budzianowski WM. An oxy-fuel mass-recirculating process for H<sub>2</sub> production  
634 with CO<sub>2</sub> capture by autothermal catalytic oxyforming of methane.  
635 International Journal of Hydrogen Energy 2010;35:7454-7469
- 636 [10] Seepana S, Jayanti S. Steam-moderated oxy-fuel combustion. Energy  
637 Conversion and Management 2010;51: 1981-1988.
- 638 [11] Toftegaard MB, Brix J, Jensen PA, Glarborg P, Jensen AD. Oxy-fuel  
639 combustion of solid fuels. Progress in Energy and Combustion Science  
640 2010;36:581-625
- 641 [12] Wang L, Liu Z, Chen S, Zheng, CG, Li J. Physical and Chemical Effects of CO<sub>2</sub>  
642 and H<sub>2</sub>O Additives on Counter flow Diffusion Flame Burning Methane. Energy  
643 Fuels 2013;27: 7602-7611
- 644 [13] Zou C, Song Y, Li G, Cao S, He Y, Zheng, CG. The Chemical Mechanism  
645 of Steams Effect on the Temperature in Methane Oxy-Steam Combustion.  
646 International Journal of Heat and Mass Transfer 2014; 75: 12-18.
- 647 [14] Perrone D. A Study of an oxy-coal combustion with wet recycle using CFD  
648 modelling. Energy Procedia 2015;82: 900- 907

- 649 [15] Yi B, Zhang L, Huang F, Mao Z, Zheng C. Effect of H<sub>2</sub>O on the combustion  
650 characteristics of pulverized coal in O<sub>2</sub>/CO<sub>2</sub> atmosphere. *Applied Energy* 2014;  
651 132: 349-357
- 652 [16] Mao Z, Zhang L, Zhu X, Pan C, Yi B, Zheng C. Modeling of an oxy-coal flame  
653 under a steam-rich atmosphere. *Applied Energy* 2016;161: 112-123.
- 654 [17] Sabia P, Lavadera ML, Giudicianni P, Sorrentino G, Ragucci R, Joannon de  
655 M. CO<sub>2</sub> and H<sub>2</sub>O effect on propane auto-ignition delay times under mild  
656 combustion operative conditions. *Combustion and Flame* 2015;162: 533-543.
- 657 [18] Tu Y, Liu H, Su K, Chen S, Liu Z, Zheng C, Li W. Numerical study of  
658 H<sub>2</sub>O addition effects on pulverized coal oxy-MILD combustion. *Fuel Processing  
659 Technology* 2015;138 :252-262
- 660 [19] Tu Y, Su K, Liu H, Chen S, Liu Z, Zheng C. Physical and Chemical Effects  
661 of CO<sub>2</sub> Addition on CH<sub>4</sub>/H<sub>2</sub> Flames on a Jet in Hot Coflow (JHC) Burner.  
662 *Energy Fuels* 2016; 30: 1390-1399
- 663 [20] Dally BB, Karpetsis AN, Barlow R S. Structure of turbulent non-premixed jet  
664 flames in a diluted hot coflow. *Proceedings of the Combustion Institute* 2002;  
665 29: 1147-1154.
- 666 [21] Oldenhof E, Tummers MJ, van Veen EH, Roekaerts DJEM. Role of entrainment  
667 in the stabilisation of jet-in-hot-coflow flames. *Combustion and Flame*  
668 2011;158:1553-1563
- 669 [22] De A, Oldenhof E, Sathiah P, Roekaerts D. Numerical simulation of delft-  
670 jet-in-hot-coflow (djhc) flames using the eddy dissipation concept model

- 671 for turbulence-chemistry interaction. *Flow, Turbulence and Combustion*  
672 2011;87:537-567
- 673 [23] Fluent Inc, *Fluent 6.3 Users Guide*, 2003.
- 674 [24] Smith GP, Golden DM, Frenklach M, Moriarty NW, Eiteneer B, Goldenberg  
675 M. *GRI-Mech 3.0*, 1999, [http://www.me.berkeley.edu/gri\\_mech/](http://www.me.berkeley.edu/gri_mech/)
- 676 [25] Chen S, Mi J, Liu H, Zheng CG. First and second law analysis of hydrogen-air  
677 counter-flow diffusion combustion in various combustion modes. *International*  
678 *Journal of Hydrogen Energy* 2012;37: 5234-5245
- 679 [26] Medwell PR, Kalt PAM, Dally BB. Simultaneous imaging of OH, formaldehyde,  
680 and temperature of turbulent nonpremixed jet flames in a heated and diluted  
681 coflow. *Combust Flame* 2007;148:48-61.
- 682 [27] Afarin Y, Tabejamaat S. Effect of hydrogen on H<sub>2</sub>/CH<sub>4</sub> flame structure of MILD  
683 combustion using the LES method. *International Journal of Hydrogen Energy*  
684 2013;38: 3447-3458
- 685 [28] Tu Y, Liu H, Chen S, Liu Z, Zhao H, Zheng C. Effects of furnace chamber  
686 shape on the MILD combustion of natural gas. *Applied Thermal Engineering*  
687 2015;76:64-75
- 688 [29] Wang F, Mi J, Li P, Zheng C. Diffusion flame of a CH<sub>4</sub>/H<sub>2</sub> jet in hot low-oxygen  
689 coflow. *International Journal of Hydrogen Energy* 2011;36:9267-9277.
- 690 [30] Weber R, Smart JP, vd Kamp W. On the (MILD) combustion of gaseous,  
691 liquid, and solid fuels in high temperature preheated air. *Proceedings of the*  
692 *Combustion Institute* 2005;30: 2623-2629



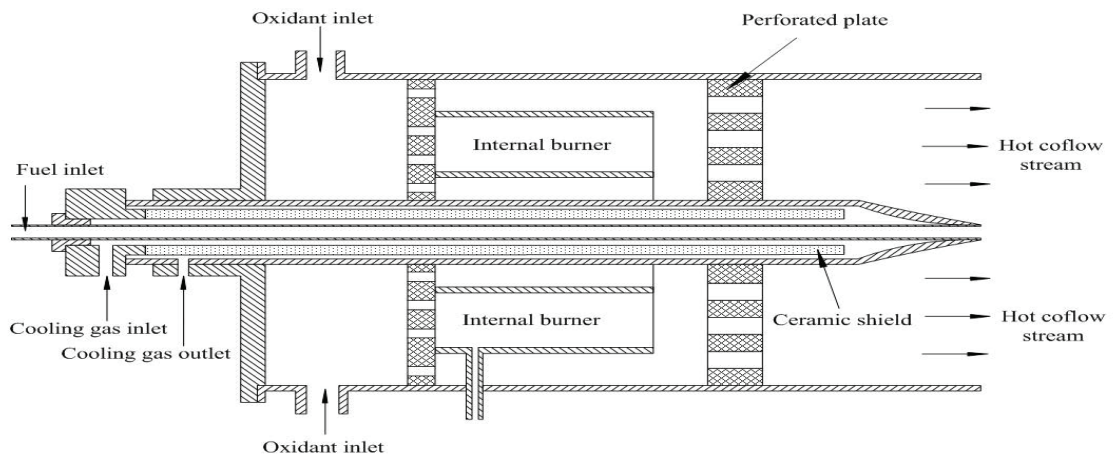


Fig. 1. Configuration of the JHC burner proposed in Ref. [20].

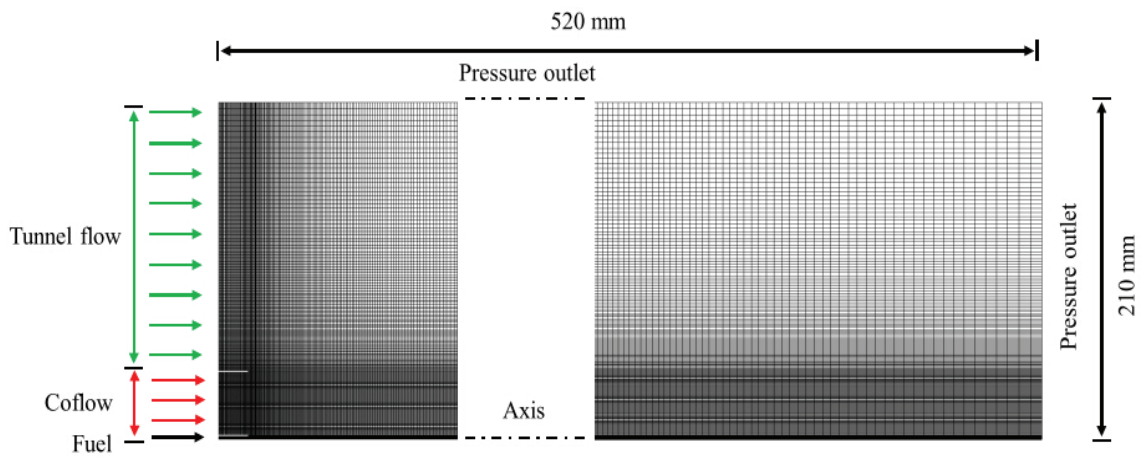


Fig. 2. Schematic configuration and coordinate system of the computational domain.

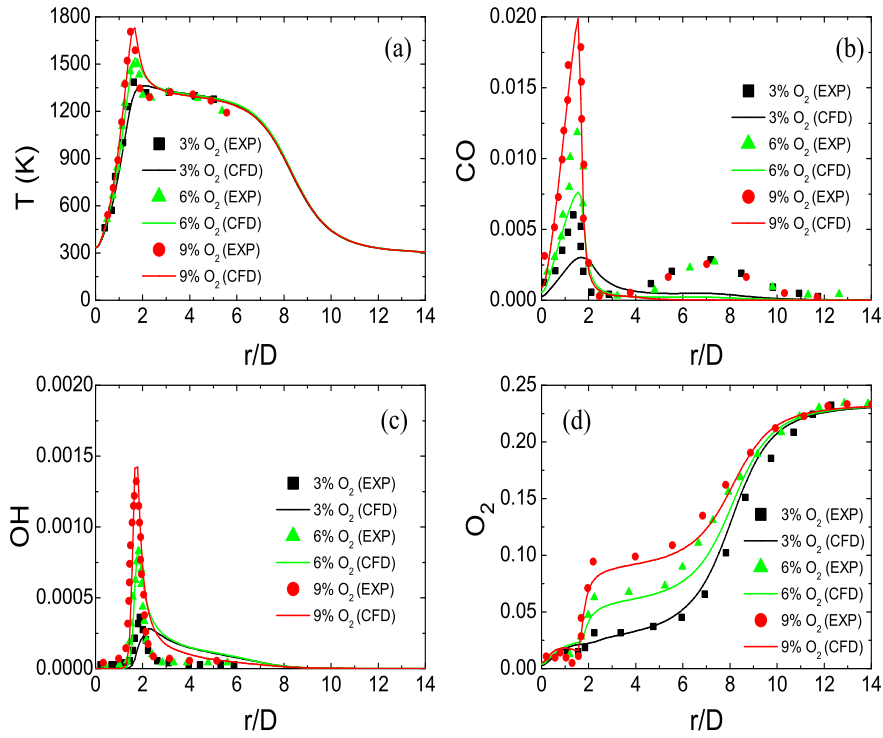


Fig. 3. comparison of (a) temperature, (b) CO mass fraction, (c) OH mass fraction, (d) O<sub>2</sub> mass fraction profiles between the present numerical prediction (CFD) and the experimental measurements (EXP) for JHC air MILD combustion with 3%, 6%, and 9% oxygen mass fraction in the co-flow at the axial location  $x = 30$  mm [20].

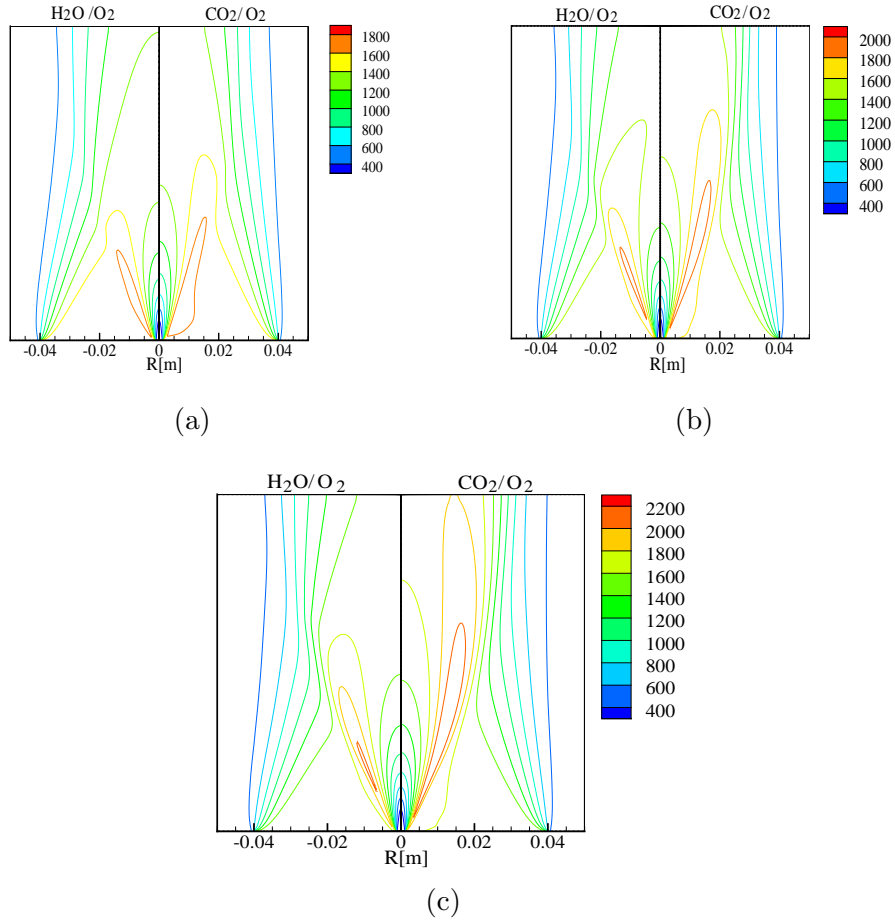
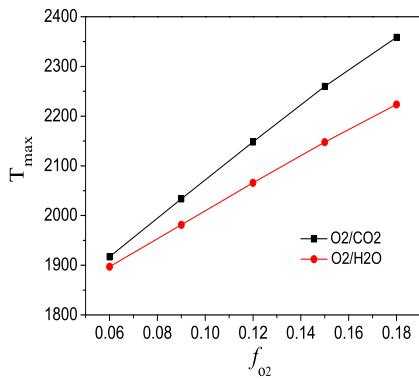
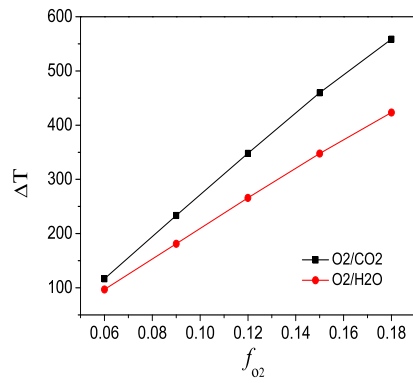


Fig. 4. Temperature distribution in O<sub>2</sub>/H<sub>2</sub>O or O<sub>2</sub>/CO<sub>2</sub> condition at (a)  $f_{O_2} = 6\%$  (b)  $f_{O_2} = 12\%$  and (c)  $f_{O_2} = 18\%$  :  $T_{cof} = 1800$  K.



(a)



(b)

Fig. 5. Maximum temperature (a) and temperature rise (b) at various  $f_{o_2}$  and  $T_{cof} = 1800$  K.

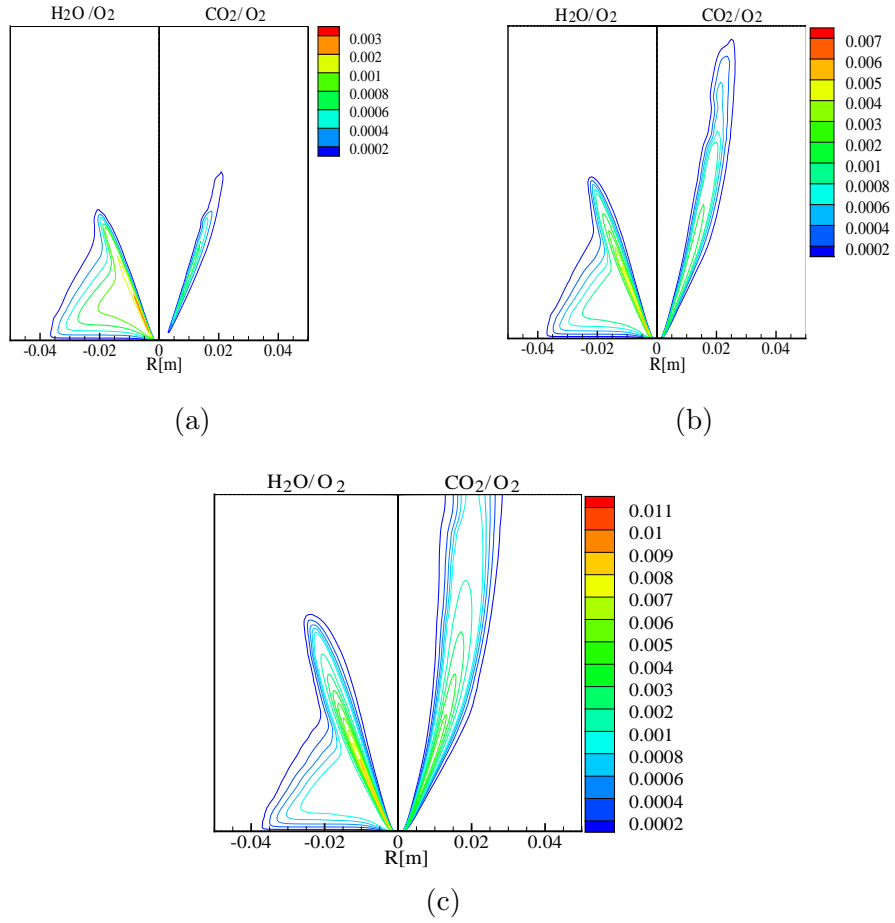


Fig. 6. OH distribution in O<sub>2</sub>/H<sub>2</sub>O or O<sub>2</sub>/CO<sub>2</sub> condition at (a)  $f_{O_2} = 6\%$  (b)  $f_{O_2} = 12\%$  and (c)  $f_{O_2} = 18\%$  and  $T_{cof} = 1800$  K.

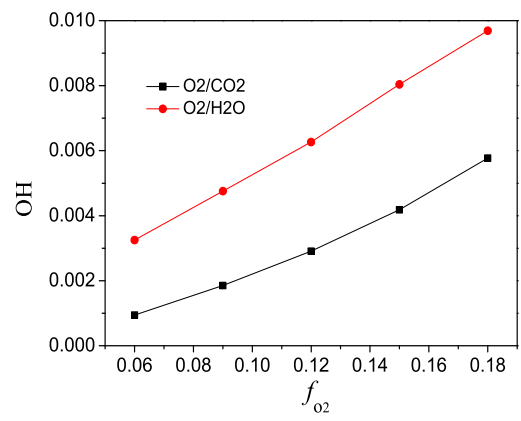


Fig. 7. The maximum of OH concentration at various  $f_{O_2}$  and  $T_{cof} = 1800$  K.

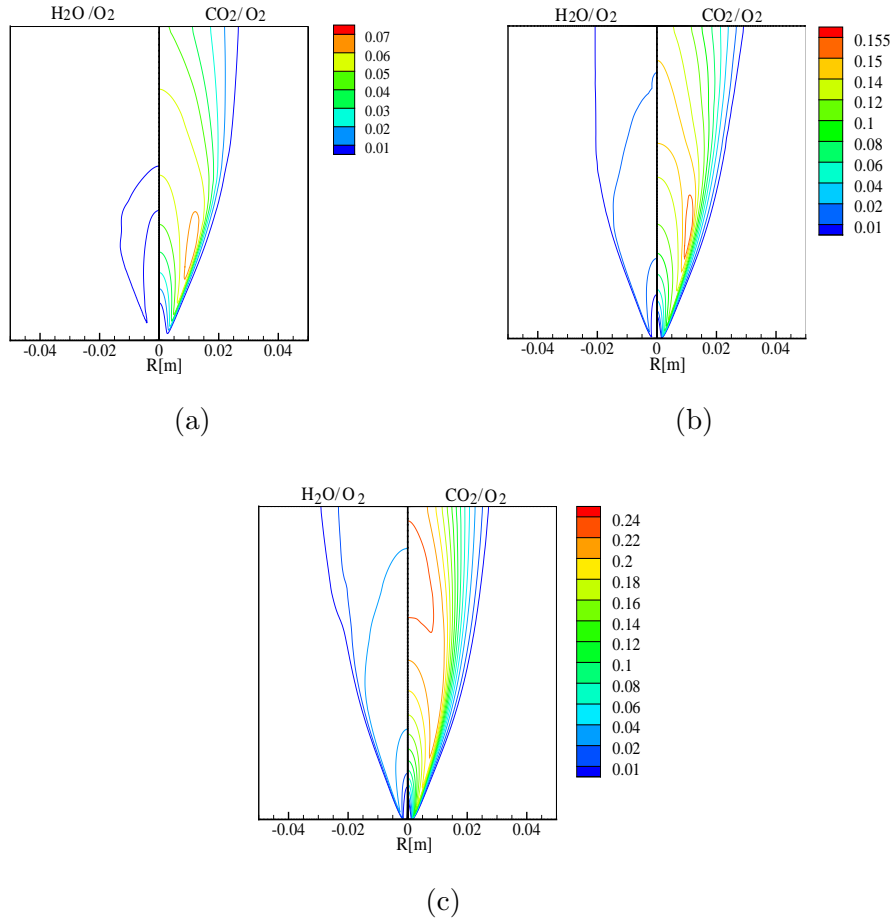


Fig. 8. CO distribution in  $O_2/H_2O$  or  $O_2/CO_2$  condition at (a)  $f_{O_2} = 6\%$  (b)  $f_{O_2} = 12\%$  and (c)  $f_{O_2} = 18\%$  and  $T_{cof} = 1800$  K.



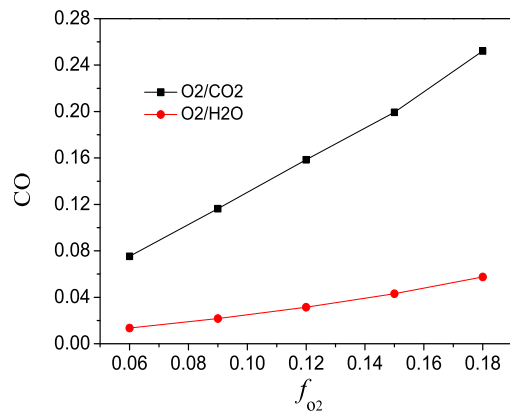


Fig. 9. The maximum of CO concentration at various  $f_{o_2}$  and  $T_{cof} = 1800$  K.

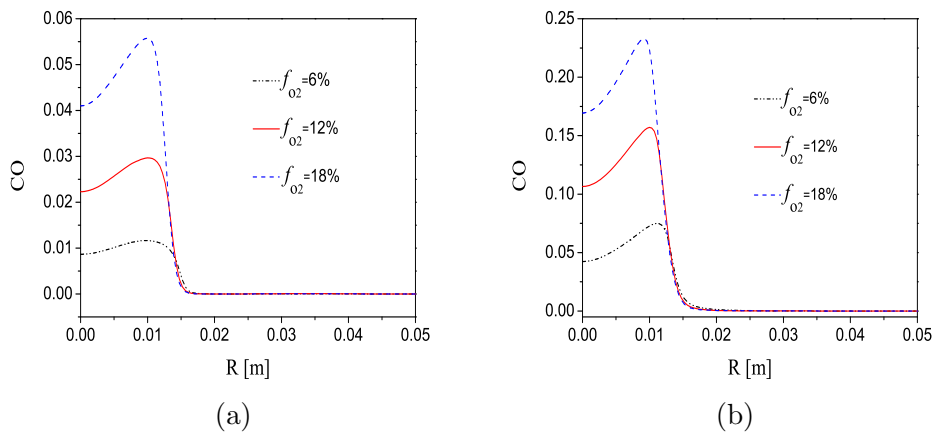


Fig. 10. CO profile in (a)  $O_2/H_2O$  and (b)  $O_2/CO_2$  condition at  $x = 90$  mm and  $T_{cof} = 1800$  K.

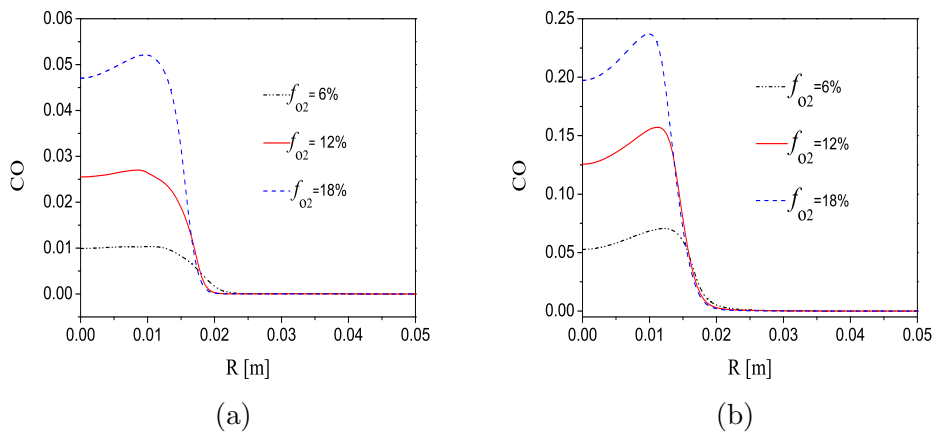


Fig. 11. CO profile in (a)  $O_2/H_2O$  and (b)  $O_2/CO_2$  condition at  $x = 120$  mm and  $T_{cof} = 1800$  K.

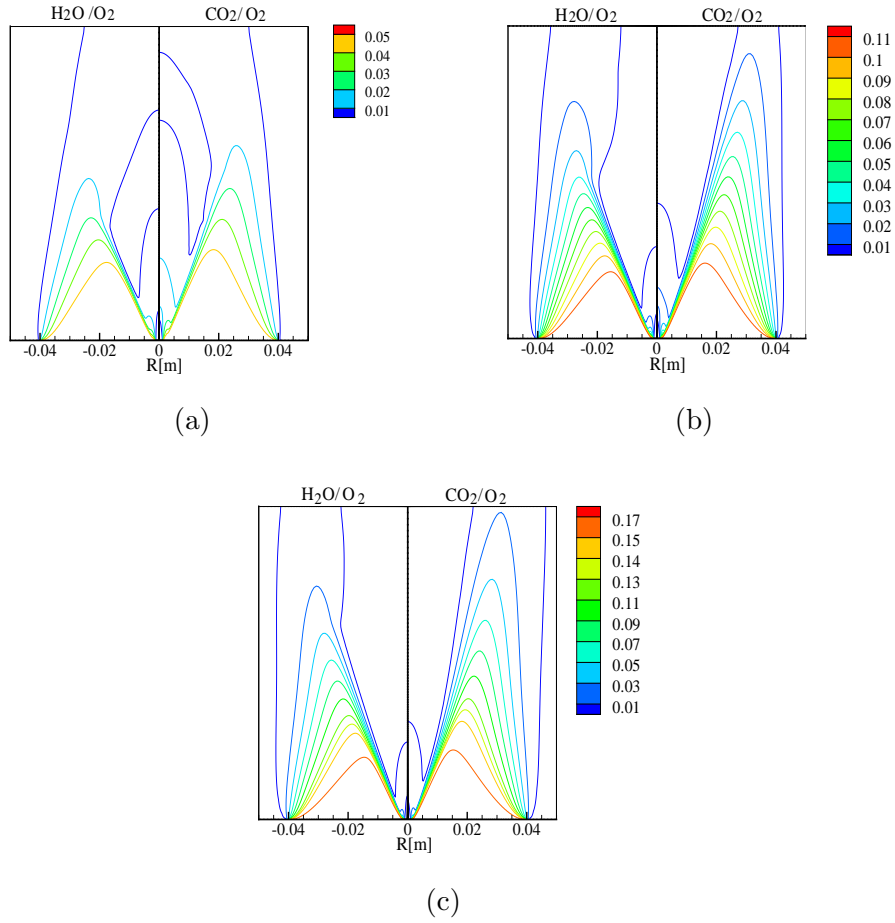


Fig. 12. O<sub>2</sub> distribution in O<sub>2</sub>/H<sub>2</sub>O or O<sub>2</sub>/CO<sub>2</sub> condition at (a)  $f_{o_2} = 6\%$  (b)  $f_{o_2} = 12\%$  and (c)  $f_{o_2} = 18\%$  and  $T_{cof} = 1800$  K.

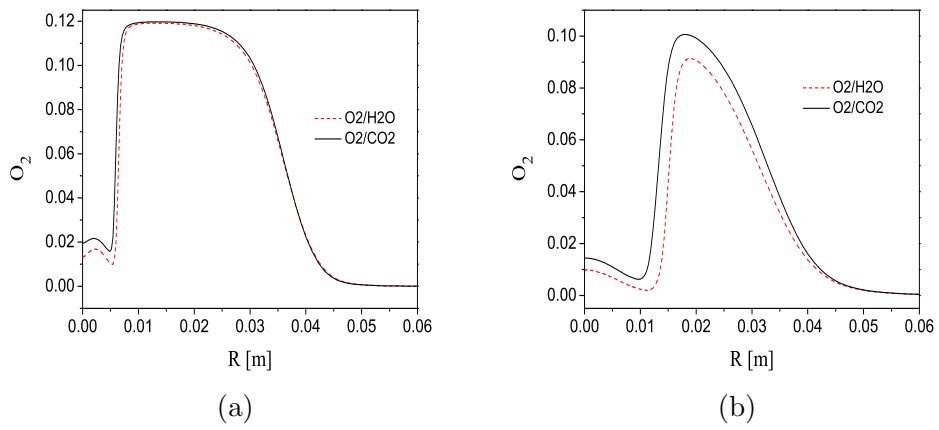


Fig. 13.  $O_2$  profile at (a)  $x = 30$  mm and (b)  $x = 90$  mm :  $f_{O_2} = 12\%$  and  $T_{cof} = 1800$  K.

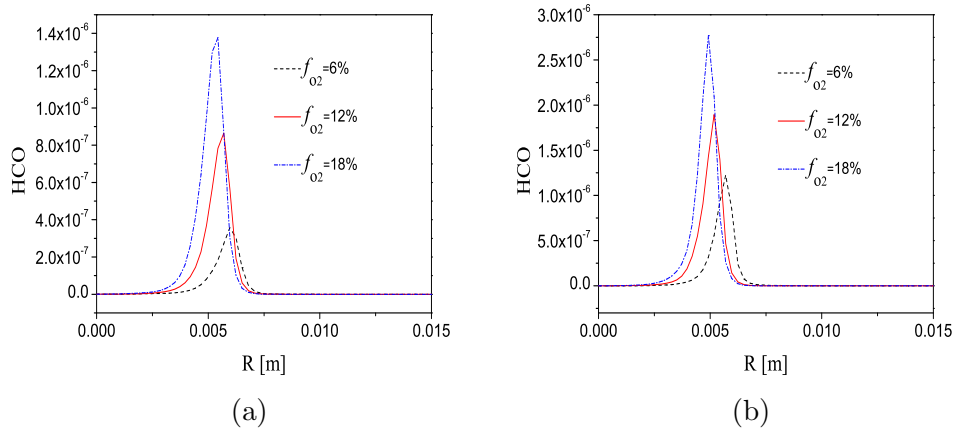


Fig. 14. HCO profile in (a)  $O_2/H_2O$  and (b)  $O_2/CO_2$  condition at  $x = 30$  mm and  $T_{cof} = 1800$  K.

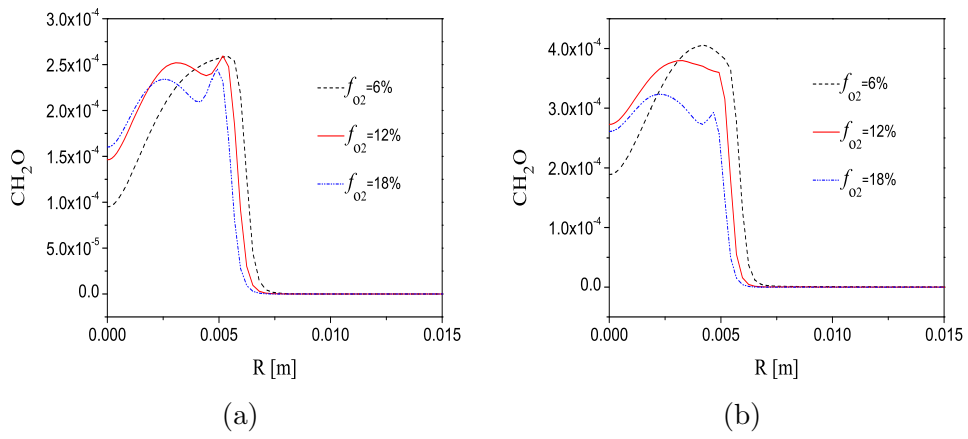


Fig. 15.  $\text{CH}_2\text{O}$  profile in (a)  $\text{O}_2/\text{H}_2\text{O}$  and (b)  $\text{O}_2/\text{CO}_2$  condition at  $x = 30$  mm and  $T_{\text{cof}} = 1800$  K.

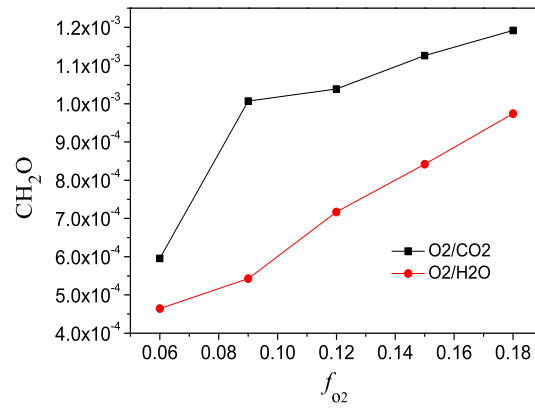
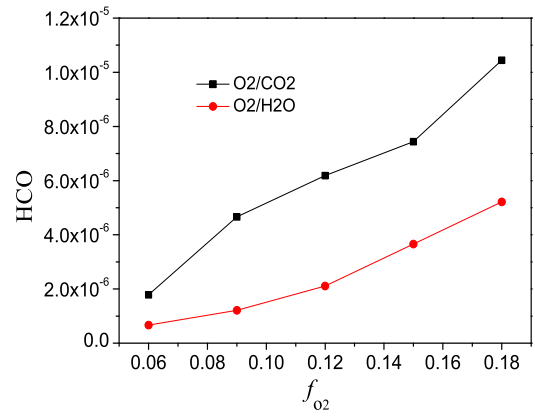


Fig. 16. The maximum of HCO (a) and CH<sub>2</sub>O (b) concentration at various  $f_{O_2}$  and  $T_{cof} = 1800$  K.



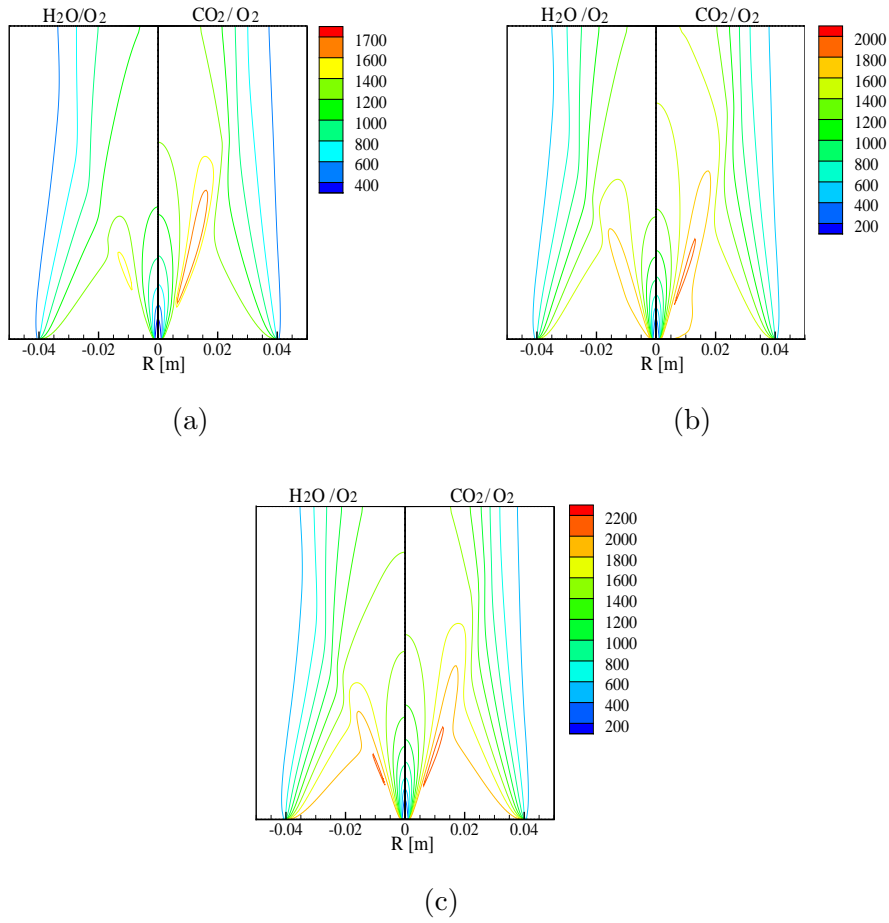


Fig. 17. Temperature distribution in  $O_2/H_2O$  or  $O_2/CO_2$  condition at (a)  $T_{cof} = 1500$  K (b)  $T_{cof} = 1800$  K and (c)  $T_{cof} = 2100$  K:  $f_{o_2} = 9\%$ .

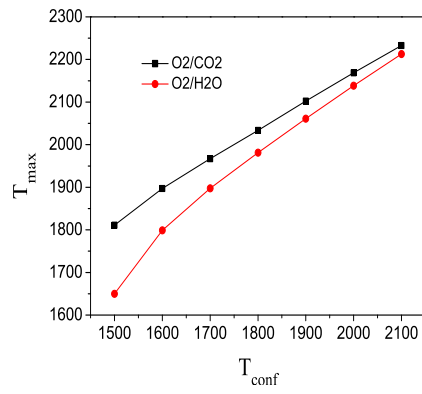


Fig. 18. Maximum temperature at various  $T_{\text{conf}}$  and  $f_{\text{O}_2} = 9\%$ .

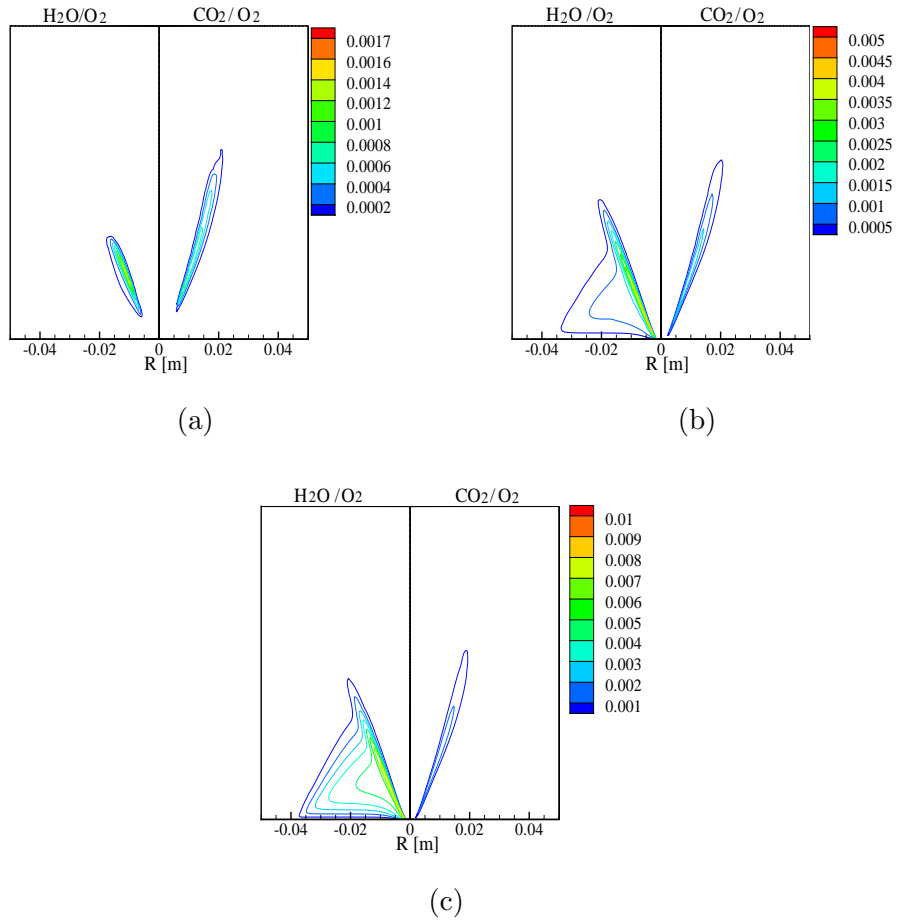


Fig. 19. OH distribution in  $O_2/H_2O$  or  $O_2/CO_2$  condition at (a)  $T_{cof} = 1500$  K (b)  $T_{cof} = 1800$  K and (c)  $T_{cof} = 2100$  K:  $f_{o_2} = 9\%$ .

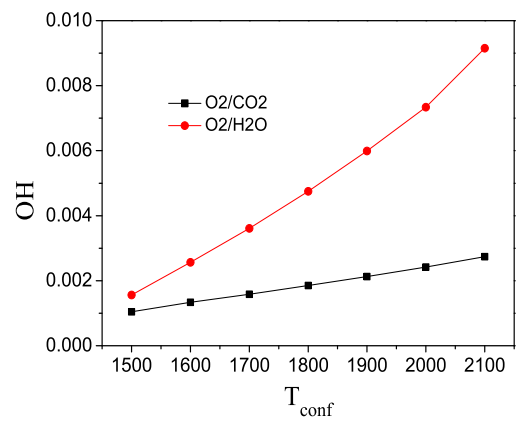


Fig. 20. The maximum of OH concentration at various  $T_{conf}$  and  $f_{o_2} = 9\%$ .

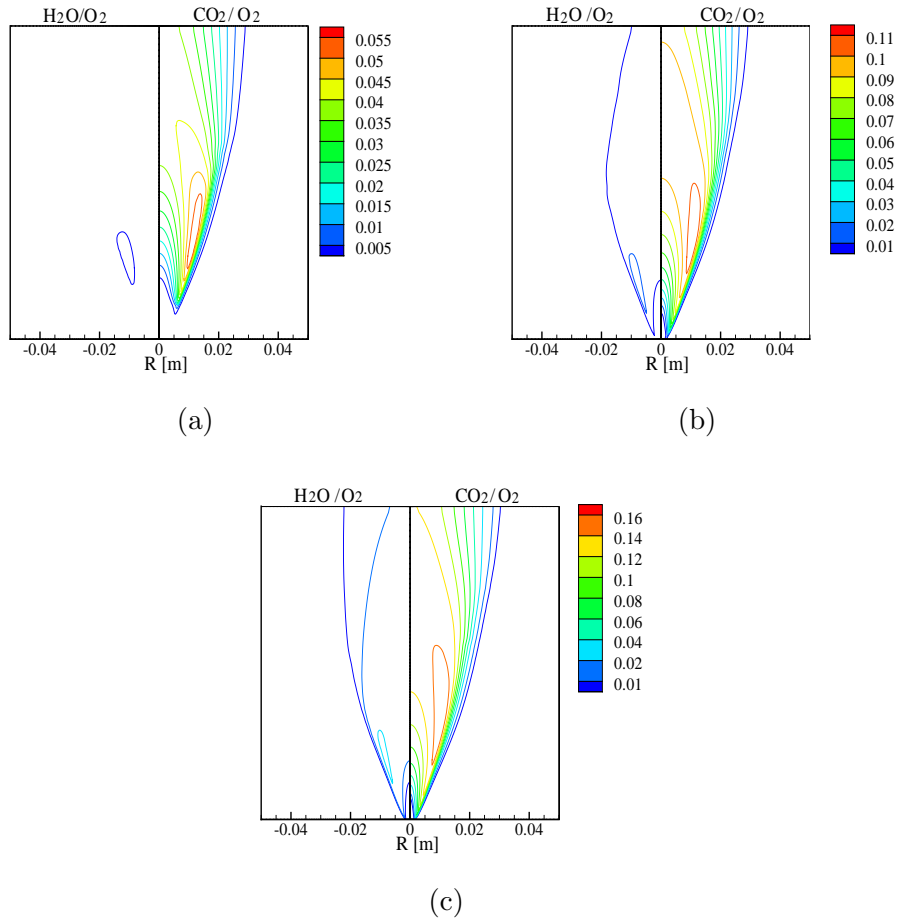


Fig. 21. CO distribution in  $\text{O}_2/\text{H}_2\text{O}$  or  $\text{O}_2/\text{CO}_2$  condition at (a)  $T_{cof} = 1500$  K (b)  $T_{cof} = 1800$  K and (c)  $T_{cof} = 2100$  K:  $f_{o_2} = 9\%$ .

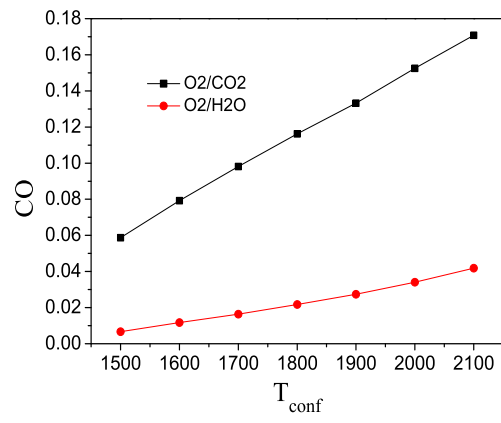


Fig. 22. The maximum of CO concentration at various  $T_{\text{conf}}$  and  $f_{\text{O}_2} = 9\%$ .

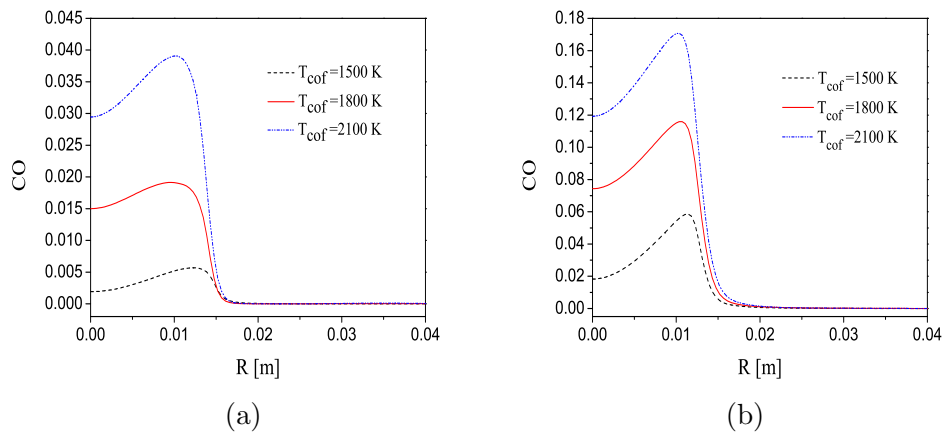


Fig. 23. CO profile in (a)  $O_2/H_2O$  and (b)  $O_2/CO_2$  condition at  $x = 90$  mm and  $f_{O_2} = 9\%$ .

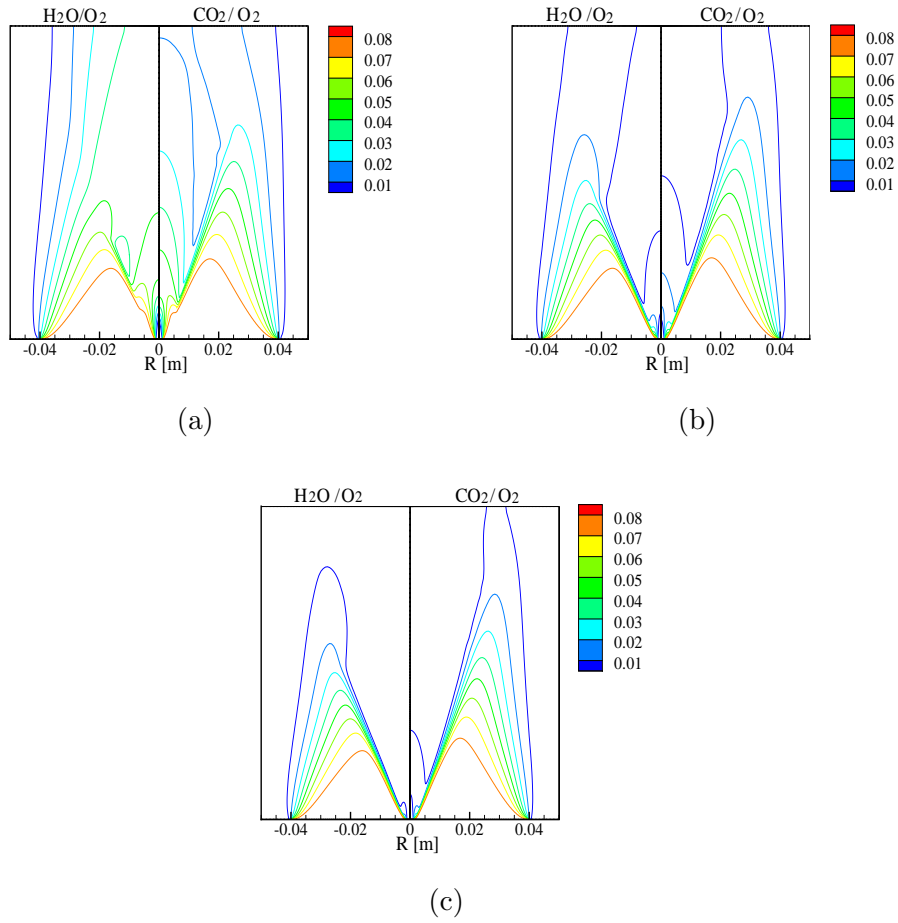


Fig. 24. O<sub>2</sub> distribution in O<sub>2</sub>/H<sub>2</sub>O or O<sub>2</sub>/CO<sub>2</sub> condition at (a)  $T_{cof} = 1500$  K (b)  $T_{cof} = 1800$  K and (c)  $T_{cof} = 2100$  K:  $f_{o_2} = 9\%$ .



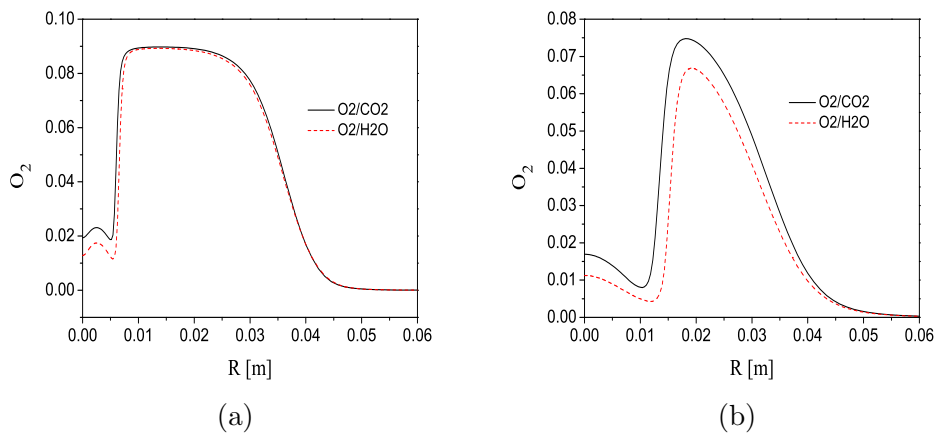


Fig. 25.  $O_2$  profile at (a)  $x = 30$  mm and (b)  $x = 90$  mm :  $f_{O_2} = 9\%$  and  $T_{cof} = 2100$  K.

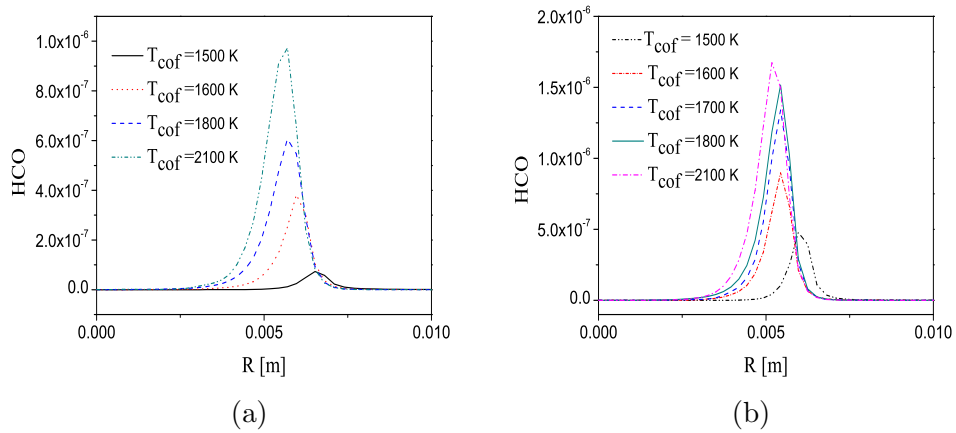


Fig. 26. HCO profile in (a)  $O_2/H_2O$  and (b)  $O_2/CO_2$  condition at  $x = 30$  mm and  $f_{O_2} = 9\%$ .

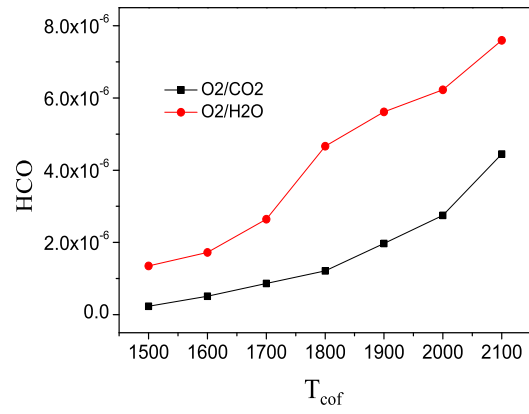


Fig. 27. The maximum of HCO concentration at various  $T_{cof}$  and  $f_{o_2} = 9\%$ .

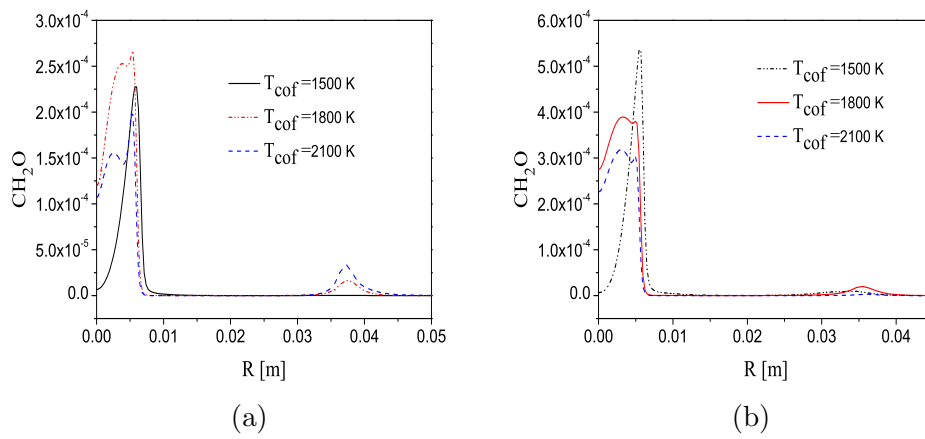


Fig. 28.  $\text{CH}_2\text{O}$  profile in (a)  $\text{O}_2/\text{H}_2\text{O}$  and (b)  $\text{O}_2/\text{CO}_2$  condition at  $x = 30$  mm and  $f_{\text{O}_2} = 9\%$ .

Table 1

Computational conditions of the present work.

Case	Fuel Flow			Co-flow					Tunnel Flow			
	$\mathbf{u}$ (m/s)	T (K)	CH <sub>4</sub> (%)	$\mathbf{u}$ (m/s)	T (K)	O <sub>2</sub> (%)	H <sub>2</sub> O (%)	CO <sub>2</sub> (%)	$\mathbf{u}$ (m/s)	T (K)	H <sub>2</sub> O (%)	CO <sub>2</sub> (%)
O <sub>2</sub> /H <sub>2</sub> O	60	305	100	3.2	1500 / 2100	6 / 18	82 / 94	0	3.2	400	100	0
O <sub>2</sub> /CO <sub>2</sub>	60	305	100	3.2	1500 / 2100	6 / 18	0	82 / 94	3.2	400	0	100